DNA Methylome Alterations are Associated with Airway Macrophage Differentiation and Phenotype During Lung Fibrosis

Peter McErlean[1], Christopher G. Bell[2], Richard J. Hewitt[1,3], Zabreen Busharat[1], Patricia P. Ogger[1], Poonam Ghai[1], Gesa J. Albers[1], Emily Calamita[1], Shaun Kingston[3], Philip L. Molyneaux[1,3], Stephan Beck[4], Clare M. Lloyd[1], Toby M. Maher[1,3,5*‡&], Adam J Byrne[1*]

[1]Inflammation, Repair and Development Section, National Heart and Lung Institute, Imperial College, London SW7 2AZ, UK.

[2]William Harvey Research Institute, Barts & The London School of Medicine, Queen Mary University of London, Charterhouse Square, London EC1M 6BQ, UK

[3]National Institute for Health Research (NIHR) Respiratory Biomedical Research Unit, Royal Brompton Hospital, Sydney Street, London SW3 6NP, UK.

[4]Department of Cancer Biology, UCL Cancer Institute, University College London, Paul O'Gorman Building, 72 Huntley Street, London WC1E 6BT, UK.

[5]Hastings Centre for Pulmonary Research and Division of Pulmonary, Critical Care and Sleep Medicine, Keck School of Medicine, University of Southern California, Los Angeles, USA.

& Associate Editor, AJRCCM (participation complies with American Thoracic Society requirements for recusal from review and decisions for authored works).

‡Correspondence:

Toby M. Maher, MD, PhD

Keck School of Medicine of USC

AJRCCM Articles in Press. Published July 19, 2021 as 10.1164/rccm.202101-0004OC

University of Southern California

2020 Zonal Ave

Los Angeles, CA 90033

t.maher@imperial.ac.uk

*Authors contributed equally

Acknowledgments:

The authors would like to acknowledge the support of the Imperial College South Kensington flow cytometry facility, particularly Ms. Jane Srivastava and Dr. Jessica Rowley. We wish to thank Dr Mark Kristiansen and Gaganjit Kaur Madhan at University College London Genomics for processing EPIC arrays. We thank Dr Michael Scherer at Department of Genetics/Epigenetics, Saarland University, Germany for advice with RnBeads analysis and providing additional code.

Funding:

P. McErlean is the recipient of the NHLI Pilot Award. A.J. Byrne is supported by a Joan Bending, Evelyn Bending, Mervyn Stephens and Olive Stephens Memorial Fellowship (AUK-SNF-2017-381). T.M. Maher is supported by a National Institute for Health Research Clinician Scientist Fellowship (ref. CS-2013-13-017) and a British Lung Foundation Chair in Respiratory Research (C17-3). C.M. Lloyd is a Wellcome Trust Senior Fellow in Basic Biomedical Science (107059/Z/15/Z**).**

Author contributions:

P. McErlean, A.J. Byrne, C.M. Lloyd and T.M. Maher designed the study. R.J. Hewitt, P.L. Molyneaux, and T.M. Maher consented patients and carried out bronchoscopies.

AJRCCM Articles in Press. Published July 19, 2021 as 10.1164/rccm.202101-0004OC

P.P. Ogger, P. Ghai, S. Kingston, G. Albers, E. Calamita and P. McErlean processed samples and gene expression analysis. P. McErlean, C.G. Bell, Z. Busharat and S. Beck analysed and interpreted DNA methylation data. All authors were involved in the interpretation of the results and drafting and/or revising the manuscript, provided final approval, and vouch for the content of the final manuscript.

Some of the results of these studies have been previously reported in the form of a preprint (bioRxiv, [04 December 2020] https://doi.org/10.1101/2020.12.04.410191)

This article has an online data supplement, which is accessible from this issue's table of content online at www.atsjournals.org.

At a Glance

Scientific Knowledge on the Subject

Airway macrophages (AMs) are key in the maintenance and defence of the airways and are implicated in the pathogenesis of idiopathic pulmonary fibrosis (IPF), a deadly respiratory disease with no cure. However, little is known of the epigenetics of AMs in health and disease.

What This Study Adds to the Field

We investigated the epigenetics of AMs by profiling DNA methylation (DNAm) in primary AMs obtained from IPF patients and healthy donors. Our work revealed that AM epigenetic heterogeneity was a key feature of AMs from IPF donors, and 'epigenetic clock' analysis revealed that these epigenetic changes were not associated with accelerated ageing (a finding in contrast to many other age-related morbidities). Furthermore, we found IPF-associated changes in AM-DNAm that

AJRCCM Articles in Press. Published July 19, 2021 as 10.1164/rccm.202101-0004OC

encompassed genes and pathways pertinent to macrophage biology and IPF pathogenesis. Importantly, epigenetic changes in genes involved in lipid and glucose metabolism were related to clinical features of IPF severity. Thus, our study establishes a link between the epigenome, AM metabolism and disease severity during IPF.

Keywords:

Pathogenesis

Monocytes

Epigenetics

DNA methylation

Interstitial lung disease

Abbreviations:

AMs – Airway macrophages

CpG – Cytosine-guanine dinucleotides

EWAS – Epigenome-wide association study

FVC – Forced vital capacity

HC – Healthy control

DHS - DNase-I hypersensitivity sites

DNAm – DNA methylation

DMPs – Differentially methylated positions

DMRs – Differentially methylated regions

IPF - Idiopathic pulmonary fibrosis

MyId-CpGs – Myeloid marker CpG dinucleotides

pcHiC - Promoter capture HiC

AJRCCM Articles in Press. Published July 19, 2021 as 10.1164/rccm.202101-0004OC

scRNA-Seq - Single-cell RNA sequencing

WGBS - Whole genome bisulphite sequencing

AJRCCM Articles in Press. Published July 19, 2021 as 10.1164/rccm.202101-0004OC

Abstract:

Rationale: Airway macrophages (AMs) are key regulators of the lung environment and are implicated in the pathogenesis of idiopathic pulmonary fibrosis (IPF), a fatal respiratory disease with no cure. However, knowledge of epigenetics of AMs in IPF are limited.

Methods: We undertook DNA methylation profiling using Illumina EPIC (850k) arrays in sorted AMs from Healthy (n=14) and IPF (n=30) donors. Cell-type deconvolution was performed using reference myeloid-cell DNA methylomes.

Measurements and main results: Our analysis revealed epigenetic heterogeneity was a key characteristic of IPF-AMs. DNAm 'clock' analysis indicated epigenetic alterations in IPF-AMs was not associated with accelerated ageing. In differential DNAm analysis, we identified numerous differentially methylated positions (DMPs, n=11) and regions (DMRs, n=49) between healthy and IPF AMs respectively. DMPs and DMRs encompassed genes involved in lipid (LPCAT1) and glucose (PFKFB3) metabolism and importantly, DNAm status was associated with disease severity in IPF.

Conclusions: Collectively, our data identify that changes in the epigenome are associated with development and function of AMs in the IPF lung.

AJRCCM Articles in Press. Published July 19, 2021 as 10.1164/rccm.202101-0004OC

Background:

Airway macrophages (AMs) are sentinel innate cells of the lungs contributing to homeostasis and immune response(1). Ontogeny of AMs is complex encompassing both self-renewing-fetal-derived 'resident' and monocyte-derived 'recruited' cells(2). Understanding of AM ontogeny in disease states and aging is contentious and has relied heavily on murine models. However, we recently helped clarify AM ontogeny in humans by identifying that one year post lung transplant, AMs in adults are derived exclusively from recruited peripheral monocytes(3).

The influence of the local microenvironment in shaping macrophage development and function is increasingly being appreciated(4). Responses to growth factors or inflammatory mediators can skew macrophage development as exemplified by the pro-inflammatory 'M1' and pro-wound healing 'M2' paradigm. However, *in vivo* macrophages exhibit tremendous heterogeneity in both health and diseased states(5-7), indicating a remarkable plasticity.

Key processes in macrophage development are reflected in changes to the epigenome including DNA methylation (DNAm)(8). Occurring in the context of cytosine-guanine dinucleotides (CpGs), DNAm influences chromatin accessibility, transcription factor (TF) binding and gene expression(9, 10). DNAm represents one of the most stable epigenetic marks and can be measured as a means of assessing the influence of development and diseases on the epigenome. In AMs, DNAm is altered in genetic and environmentally-induced chronic airway diseases(11-13). Regional differences in lung anatomy also influence DNAm in AMs(14), suggesting that shaping of AM development in the lung microenvironment comprises an epigenetic component. However, despite recent advances in our understanding of AM ontogeny,

AJRCCM Articles in Press. Published July 19, 2021 as 10.1164/rccm.202101-0004OC

the epigenetics of monocyte to macrophage development in the lung and influence of disease on these processes remain limited.

Idiopathic pulmonary fibrosis (IPF) is a deadly respiratory disease of unknown aetiology with heterogeneous cellular and molecular mechanisms(15). The pathobiology of IPF is characterised by a pro-fibrotic wound-healing cascade that does not resolve, leading to progressive scarring, loss of lung function and ultimately death(16). Although containing a strong genetic component(17), the greatest risk factor for IPF is age (median 65 years(18)) and prognosis in IPF is worse than some cancers with a mean survival of 3-5 years(19). In the IPF lung, AMs exhibit transcriptional(7), immuno-phenotypic(1) and metabolic differences(20, 21). Recent studies employing single-cell RNA sequencing (scRNA-Seq) have indicated a transcriptional spectrum of AMs in the IPF lung that reflects facets of both M1 and M2 macrophage paradigm(5-7). However, despite their emerging role in IPF pathogenesis, the molecular mechanisms underlying transcriptional and other phenotypic characteristics of AMs in IPF are poorly understood.

In the current study we investigated the epigenetics of AMs by undertaking genome-wide DNAm profiling using the Illumina EPIC (850k) arrays. By comparing AMs and other myeloid cell DNA methylomes, we sought to clarify the epigenetics of AM development in the lung. By profiling AMs from healthy and IPF donors, we also sought to determine if changes in the epigenome characterize features of AMs observed in the IPF lung.

AJRCCM Articles in Press. Published July 19, 2021 as 10.1164/rccm.202101-0004OC

Results:

The DNA methylation profile of AMs is distinct from that of peripheral monocytes or cultured macrophages:

Given recent work identifying AMs as monocyte-derived and having characteristics spanning the M1-M2 spectrum of activation, we sought to determine if these changes are also reflected at the epigenetic level by comparing the DNA methylome in AMs and other myeloid cells.

Firstly, we enriched CD206+ AMs, obtained through bronchoalveolar lavage, from healthy (n=14) and IPF (n=30) donors and assayed DNAm using Illumina Methylation EPIC (850k) arrays, which interrogate >850,000 CpGs across the genome with an enrichment for functional loci (promoters and enhancers, Table 1)(22). These data were then merged with whole genome bisulphite sequencing (WGBS) Blueprint datasets from representative myeloid cell-types including CD14+CD16- 'Classical' and CD14+CD16+ 'Other' monocytes and *in vitro*-derived M0, M1, and M2 macrophages(23) (Figure 1A). We then identified the top 500 CpGs with a DNAm profile which best discriminated each monocyte and macrophage subtype (see methods) and characterized these as 'myeloid marker CpGs' (myld-CpGs, Table S1).

We found that myld-CpGs reside predominately in intronic and intergenic regions (Figure 1B) that are enriched for other epigenetic features in myeloid cells including histone modifications indicative of poised enhancers (H3K4me1 without H3K27ac) and open chromatin (DNase-I hypersensitivity sites: DHS, Figure 1C-D). Functional enrichment analysis additionally indicated that myld-CpGs encompass a diverse range of receptor signalling, immune cell activation, chemokine and metabolic-related processes and pathways (Figure 1E). Although annotated to n=449 genes, we found

AJRCCM Articles in Press. Published July 19, 2021 as 10.1164/rccm.202101-0004OC

AT-Rich Interaction Domain 5B (*ARID5B*), a transcriptional co factor which has been shown to regulate glucose metabolism(24), contained the most myld-CpGs (Figure 1F, Table S1)

We focused further on *ARID5B* and mining scRNA-Seq datasets from healthy and diseased lung (IPF/COPD) established that *ARID5B* is expressed across immune cells including monocytes and macrophages (Figure S1A). At the *ARID5B* locus we found that the myld-CpGs are clustered at the promoter region of a shorter transcript variant 2 and overlap with DHS and H3K4me1 enrichment (Figure 1G). We then confirmed the expression of the shorter *ARID5B* transcript in AMs and the M1 macrophage subset (Figure S1B-C). Finally, closer inspection revealed dramatic changes in DNAm towards the shorter *ARID5B* variant promoter region with AMs exhibiting an intermediate DNAm profile (avg. 50.8%) compared to other myeloid cells (monocytes - avg. 85.4% and macrophages - avg. 0.6%, Table S1). Taken together, these results indicate that the DNAm profile of human AMs is distinct from that of peripheral monocytes/cultured macrophages and we identify *ARID5B* DNAm status as a marker of AM development.

Changes in the AM-methylome define IPF-AMs:

Next, to determine whether the methylome was distinct in each cell-type or disease state, we clustered DNAm profiles for genes with >2 myld-CpGs. Interestingly, our analysis indicated that epigenetic heterogeneity is a feature of IPF, as DNAm profiles across myld-CpGs were distinct when comparing healthy and IPF AMs (Figure S1D). Furthermore, the DNAm of AMs overlapped significantly with other myeloid cells, potentially indicating monocytic origin.

AJRCCM Articles in Press. Published July 19, 2021 as 10.1164/rccm.202101-0004OC

To clarify this further we performed deconvolution analysis of AM DNAm datasets with mlyd-CpGs (see methods). Deconvolution revealed that while at the epigenetic level healthy and IPF AMs were predicted to be largely a composite of 'other' monocytes and M0/M2 macrophages, clustering identified the separation of healthy and IPF AMs (Figure 2A), driven largely by differences in the minor classical monocyte and M1 macrophage fractions (Figure 2B). However, further investigation revealed that the specific differences in subsets was related to donor age (Figures 2C).

Because IPF and ageing are linked and many age-related diseases exhibit 'accelerated' changes to the epigenome, we next used DNAm 'clock' analyses to clarify the contribution of ageing towards the predicted myeloid cell composition of AMs. Epigenetic 'clocks' use changes in DNAm to estimate sample donor age. Specifically, the 'clocks' are constructed using elastic net regression to parsimoniously reflect the ageing-related DNA methylome changes with a very small set of CpGs (e.g. Horvath = 355 CpGs, Hannum et al. 71 CpGs)(25). The 'clocks' provide a strongly validated age in years estimate and, subsequently, have led to the observation of an older prediction than actual chronologic age, or positively 'accelerated' ageing, with a number of specific diseases(26-28) as well as morbidity and mortality(29). Age-adjusted clock results were adjusted for chronological age by forming a residual and then compared by t-tests (see Methods). We found that while a strong correlation between chronological and epigenetic age was present for the blood and tissue-derived Hannum and Horvath 'clocks' respectively (Figure 2D and S1E), no differences in age-adjusted DNAm 'clock' age acceleration was observed between healthy and IPF AMs (Figure 2D). Furthermore, while both the Horvath and Hannum et al. clocks may underestimate the age of older individuals (>60 years) due to non-linear effects potentially driven by signal saturation (30), we also found no positive age

AJRCCM Articles in Press. Published July 19, 2021 as 10.1164/rccm.202101-0004OC

acceleration in IPF across other epigenetic clocks that are less likely to be influenced these effects (Figure S1F). This does not exclude the role of ageing-related changes, but there is no supportive evidence for an acceleration beyond chronological age of the robust ageing-related changes captured by DNA methylation 'clocks', at the power resolution of this purified cell-type study(25). Importantly, there was no relationship between predicted myeloid cell composition and epigenetic age acceleration (Figure 2E and S1G), inferring that myeloid cell composition was a feature of IPF AMs and not the more generalised DNAm 'clock' changes. Taken together, these data indicate that epigenetic heterogeneity is present in AMs and is a characteristic of IPF.

Identification of differentially methylated positions (DMPs) in IPF:

We next sought to determine whether AMs DNAm profiles are impacted during IPF and to identify the impact of myeloid cell composition in these analyses. Initial principal component analysis indicated a separation of donors by disease group (Figure S2A) with myeloid cell composition and donor age being comparable drivers of variance within the dataset (Figure S2D).

We then undertook analysis to identify DMPs in IPF, employing a robust genome-wide significance threshold P value <9x10-8 that controls for the false positive rate of the DNAm EPIC arrays (31) and observed a dramatic impact when adjusting for myeloid cell composition in addition to other study covariates (Figure 3A and methods). This was equally evident when investigating direction of DNAm change in IPF with all myeloid-adjusted DMPs identified (n= 11) losing DNAm compared to healthy controls (Figures 3B, S2C-D and Table S2).

IPF DMPs were either intronic (n=9) or intergenic (n=2) and occurred in regions enriched for open chromatin in myeloid cells (DHS, Figure S2E). We found n=3 IPF

AJRCCM Articles in Press. Published July 19, 2021 as 10.1164/rccm.202101-0004OC

DMPs clustered at Lysophosphatidylcholine Acyltransferase-1 (*LPACT1*), an enzyme which mediates the conversion of lysophosphatidylcholine to phosphatidylcholine(32) (Figure 3B). Mining of IPF scRNA-Seq data indicates that *LPCAT1* is expressed across monocytes and macrophages in the lung, and we confirmed these findings in our study AMs (Figure S2F-G).

Although *LPCAT1* DMPs are intronic, distal regions can influence gene expression through 3D interactions. To investigate this further, we used promoter capture HiC (pcHiC) data to investigate the relationship between IPF DMPs and 3D interactions in myeloid cells(33). Remarkably, while the *LPCAT1* promoter interacted with other genes/regions specifically in monocytes (Figure S2H), the strongest interaction occurred with the region containing the IPF DMPs (Figure 3C). We identified a correlation between IPF DMPs methylation and gene expression occurred only for *LPCAT1* (Figure 3D) and not any other interacting genes (Figure S2I).

Finally, we investigated the relationship between *LPCAT1* and clinical features of IPF (Table 1) and found that while no relationship was present for gene expression (Figure 3E), there was a strong correlation between methylation and forced vital capacity (FVC), a measure of disease severity and progression in IPF(34) was evident (Figure 3F). Taken together these data suggest AMs similarity to monocytes on the epigenetic and higher order 3D-interaction level and a function of DNAm of AMs in IPF pathogenesis.

Identification of differentially methylated regions (DMRs) in IPF:

Given the clustering of IPF DMPs, we next conducted analysis to identify DMRs containing changes across >3 CpGs and an FDR P<0.05 in IPF(35). Similar to DMP analysis, we saw a reduction in total DMRs identified after adjusting for myeloid cell

AJRCCM Articles in Press. Published July 19, 2021 as 10.1164/rccm.202101-0004OC

composition (Figure 4A). However, we found n=49 myeloid-adjusted DMRs which included regions both gaining and losing DNAm compared to healthy controls (Table S3). We also found n=2 DMRs which encompassed the previously identified DMPs of *LPCAT1* and DNA Polymerase Epsilon, Catalytic Subunit (*POLE*, Figure 3B).

IPF DMRs were distributed across various genomic features including promoters, introns and exons (Figure 4B), occurred in regions enriched for open chromatin in myeloid cells (Figures 4C-D) and were more likely linked in 3D to distal genes and regions (Figure S3A-C). We additionally found motifs matching TF's previously implicated in macrophage polarisation to be enriched in IPF DMRs (e.g. KLF4, FOXO1, Figure 4E) and the subsequent cell-type expression profiles of TF encoding genes across lung immune cells (Figure S3D).

While mining of scRNA-Seq data revealed only some DMR-associated genes were expressed/detected in monocyte and macrophage subsets identified in the IPF lung (Figure S3E), remarkably IPF and healthy donors clustered separately based on respective DMR-associated gene expression profiles (Figure S3F).

We then undertook functional enrichment analysis and found enrichment across various processes and pathways pertinent to macrophage biology (e.g. extravasations) and IPF pathogenesis (e.g. platelet activation, response to wound healing; Figure S4A).

To gain a better insight into the biological implications of changes in DNAm, we undertook additional protein-protein interaction analysis and found that DMR-associated genes form the central hubs of large interconnect networks (Figure 5A and Figure S4B). We refined our analysis further and undertook functional enrichment of networks by DNAm status and found hub genes gaining DNAm in IPF predominately

AJRCCM Articles in Press. Published July 19, 2021 as 10.1164/rccm.202101-0004OC

encompass metabolic processes whilst those losing DNAm play a role in processes and pathways pertinent to macrophage biology and fibrogenesis (e.g. phagocytosis, cell proliferation and TGF-β signalling, Figure 5B).

Given that work from our lab has identified an altered state of AM metabolism in IPF(20, 21), we focused on 6-Phosphofructo-2-Kinase/Fructose-2,6-Biphosphatase 3 (*PFKFB3*), a potent driver of glycolysis(36) and found the associated IPF DMR was located in an intergenic region, upstream of the *PFKFB3* promoter and overlapped H3K4me1 and DHS enrichment (Figure 5C). Remarkably, a complete loss of methylation for CpGs at the *PFKFB3* TSS was observed for study AMs and across macrophage subsets (Figure S4C-D).

We then found *PFKFB3* was differential expressed between healthy and IPF not only in our study AMs, but also across macrophages in scRNA-Seq data from the IPF lung and macrophage subsets (Figure S4E-G). We subsequently identified a correlation in AMs between DNAm and gene expression for two of the 3 CpGs encompassing the *PFKFB3* DMR (Figure 5D) and identified relationships between *PFKFB3* gene expression and methylation with severity of IPF as determined by FVC (Figure 5E-F). Taken together these data strongly suggest that changes in the epigenome underpin the distinct metabolic phenotype observed in AMs isolated from IPF lung and their contribution towards disease pathogenesis.

Discussion:

AMs are key regulators of the lung environment and are implicated in the pathogenesis of lung fibrosis. By comparison to reference myeloid cells, we determined that epigenetic heterogeneity is present in AMs and, furthermore, is a characteristic of IPF (Figure 2). While identified computationally, our findings mirror scRNA-Seq studies of

AJRCCM Articles in Press. Published July 19, 2021 as 10.1164/rccm.202101-0004OC

the IPF lung where AMs exhibit transcriptional heterogeneity(5-7). Differences in myeloid cell composition also suggests that the IPF lung influences monocyte to macrophage developmental trajectories. Interestingly, transcriptomic signatures reflective of blood monocytes are already altered in association with IPF severity(37-39), potentially indicating that the effects of IPF extends across tissue compartments rather than being isolated to the lung.

In the absence of single-cell data, computational deconvolution of epigenetic data is essential to decipher disease effects within samples consisting of mixed cell populations(40). Even though we had enriched AMs based on cell surface expression of CD206, we identified epigenetic heterogeneity and found a tremendous impact of myeloid cell composition in identification of DMPs and DMRs in IPF. Our work has implications for previous studies of DNAm in IPF that have largely assayed whole lung tissue in 'bulk' without accounting for cell-type heterogeneity(41, 42). Furthermore, our study employed a genome-wide approach, providing better insights into the influence of IPF on the wider epigenome than previously conducted gene-specific studies in this disease area (43).

Advanced age is a key risk factor for IPF(44), and numerous studies have shown that molecular changes commonly associated with aging such as telomere shortening (45, 46) and augmented markers of senescence (47, 48) are found in IPF patients. While the identification of epigenetic heterogeneity in AMs was important for deciphering DNAm changes in IPF, we additionally found that donor age correlated with this predicted heterogeneity. To address the potential interaction of heterogeneity and age, we conducted epigenetic 'clock' analysis as these signatures are actively being explored for possible novel age-related disease insights(49). However, we found no

AJRCCM Articles in Press. Published July 19, 2021 as 10.1164/rccm.202101-0004OC

differences in age acceleration between healthy and IPF AMs or relationship to predicted myeloid cell composition. These findings are in contrast to many other age-related diseases(25) and indicate that whilst IPF predominately occurs in later decades, the DNAm changes detected are likely to be specific to IPF rather than representing epigenome changes occurring as a consequence of otherwise 'healthy ageing'(50). Although these analyses and other adjustments for donor age in differential analysis revealed influence of IPF on AMs DNAm, IPF and age remain inexplicably linked. Future studies of epigenetics in IPF should therefore strive to include age and sex matched healthy controls.

In mice, recruited, monocyte-derived, as opposed to foetal-derived tissue-resident AMs, have been implicated in the pathogenesis of pulmonary fibrosis (2). However, the origins of AMs during IPF have not been defined. By attempting to clarify the epigenetic events related to macrophage development in the lung, we found that DNAm patterns which discriminate myeloid cell-type occur largely in intronic and intergenic regions. This supports previous work indicating epigenomic changes during immune cell lineage commitment occurs within non-coding regions(51). However, we identified intergenic DNAm within *ARID5B* at the promoter for a shorter transcript variant 2 as a mark of monocyte to macrophage development. *ARID5B* is a chromatin modifier that acts as a transcriptional coactivator by removing repressive histone modifications(52). Additionally, *ARID5B* has been linked to adipogenesis(53) and metabolism in hepatocytes(54) and natural killers cells, where altered DNAm particularly of the short transcript variant 2 characterized a HMCV+ adaptive NK cell subtype(55). More relevant to this study was work using a multi-omics approach that identified *ARID5B*'s association with atherosclerosis in CD14+ blood monocytes and implicated 3D interactions in linking intronic *ARID5B* DNAm (and other regulatory

AJRCCM Articles in Press. Published July 19, 2021 as 10.1164/rccm.202101-0004OC

regions) with the *ARID5B* promoter(56). Thus, our data indicate that the DNAm profile of mature AMs is distinct from that of peripheral monocytes and identify *ARID5B* DNAm as a marker of AM development.

Recently AM metabolic function has been implicated in the pathogenesis of IPF. Increased expression of the glucose transporter GLUT1 has been described in IPF-AMs(57), as well as accumulation of dysmorphic mitochondria and reduced oxidative phosphorylation-related gene expression (58). Indeed, work from our lab has indicated the crucial role of AM metabolic rewiring in IPF(20, 21). Here, our data demonstrate that aberrant AM-metabolism during IPF may be in part under epigenetic control. We identified IPF DMRs encompassed hubs genes of networks associated with lipid, iron and glycolytic metabolic processes, suggesting epigenetic control likely occurs at key genes in a discrete manner rather than across pathways or processes at large.

Indicative of the impact of changes in DNAm was the DMR located at *PFKFB3*, an enzyme responsible for the synthesis and degradation of fructose 2,6-bisphosphate, a key regulator of glycolysis. Recent work has identified an important role of *PFKFB3* in controlling macrophage plasticity and activation during liver fibrosis(59), in maintaining cell viability under hypoxic and inflammatory conditions(60), as well as promoting macrophage antiviral responses(61). Furthermore, n=3/11 EWAS DMPs in IPF clustered within an intronic region of *LPCAT*1 an evolutionarily conserved enzyme that is involved in phospholipid metabolism and performs a key role in surfactant production in alveolar type 2 cells(62) and inflation of lungs upon birth(63). Recent work has also implicated *LPCAT1* with aberrant metabolism and plasma membrane remodelling in cancer (64).

AJRCCM Articles in Press. Published July 19, 2021 as 10.1164/rccm.202101-0004OC

In IPF, reduction of *LPCAT1* gene expression was shown to characterise subsets of IPF-specific airway epithelial cells(65). Interestingly, despite not reaching EWAS significance, we observed changes in DNAm in IPF AMs at the related paralog *LPCAT2* (Figure S2J). While no difference in *LPCAT2* gene expression was observed in IPF AMs, *LPCAT2* is expressed more than *LPCAT1* across macrophage subtypes (Figure S2K-M). These data suggest that epigenetic regulation of phospholipid metabolism specifically in AMs may occur via a *LPCAT1*-dependent manner and further supports the role of discrete changes in DNAm contributing to altered lipid and other metabolic defects in IPF(57, 58, 66).

Our work has several limitations that should be considered. First, similar to work in blood monocytes(56), we investigated whether integrating 3D interactions could help elucidate the potential impact of changes in DNAm on gene expression(33). Remarkably, we found the *LPCAT1* promoter 'self-interacted' with regions containing IPF DMPs and over half of all DMRs were linked in 3D to other genomic regions in myeloid cells. While these data suggest that similar to DNAm, AMs share a higher order chromatin structure similar to monocytes and macrophages, bias from the EPIC array design needs to be taken into consideration. Future studies should therefore aim to determine 3D interactions in AMs from healthy and IPF donors empirically.

Second, given the composition of AMs in IPF was more 'M1-like' and the progressive remodelling of the IPF lung results in an inflammatory hypoxic environment, these results raise the question of whether development and epigenetic changes identified in IPF AMs are a cause or consequence of the fibrotic milieu of the IPF lung. Future studies should seek to enrich individual pulmonary cell types (as well as their circulating precursors) to assess how the duration of exposure in the IPF lung alters

AJRCCM Articles in Press. Published July 19, 2021 as 10.1164/rccm.202101-0004OC

the epigenome by comparing more transient cell types (i.e. immune) to those unable to 'escape' the hypoxic/fibrotic milieu (i.e. stromal/epithelial cells). Furthermore, while our work identifies epigenomic changes during monocyte to macrophage transition in the lung, these data are inferred from computational deconvolution of bulk populations. Future studies of IPF should seek to generate matched transcriptome and epigenomic datasets across blood and lung to comprehensively address the molecular events and influence of IPF on AM developmental trajectories.

Finally, we did not investigate avenues to recapitulate or reverse the changes in DNAm observed in our study. In addition to more traditional chemical-based methods (e.g. DNAm inhibitors), advances in epigenome-editing techniques that can effectively recapitulate diseased epigenomes *in vitro(67)* should be employed in future studies to allow functional characterization of epigenetic changes occurring in monocyte to macrophage transitions and IPF pathogenesis(68).

In conclusion, our study has identified a role of aberrant epigenetic regulation of AMs, independent of ageing alone, which appears to be involved in IPF pathogenesis. Our study provides a foundation for further investigations to clarify the role of epigenetics during monocyte to macrophage development in the healthy and diseased airways. Furthermore, our data highlight the possibility that therapeutic agents targeting epigenetic modification may have a role in the treatment of IPF.

Methods:

Patient recruitment and AM enrichment:

Study donors underwent bronchoscopy and collection of BAL as outlined previously(20, 21). All study donors provided written informed consent to participate

AJRCCM Articles in Press. Published July 19, 2021 as 10.1164/rccm.202101-0004OC

in the study, which was approved by the research ethics committee (10/HO720/12, 15/LO1399 and 15/SC/0101). Clinical characteristics of donors are outlined in Table 1. CD206+ AMs were enriched from donor BAL using the magnetic-based MACS® system (Miltenyi Biotech, Germany) and fluorescent activated cells sorting (FACS) as outlined previously(3, 20, 21).

DNA/RNA extraction and EPIC methylation arrays:

Nucleic acids were extracted from cells using the AllPrep Mini Kit (QIAGEN, Germany) and quality assessed using Genomic DNA ScreenTape and TapeStation System (Agilent, USA). DNA was submitted to the UCL Genomics Core facility for hybridization on Infinium MethylationEPIC BeadChip Arrays (Illumina, USA). We employed RnBeads 2.0 pipeline(69) for methylation array preprocessing. Briefly, quality control (QC) metrics were generated and samples passing QC were normalized using the *Dasen* function (70). Following preprosessing, n=784,669 probes for each n=44 samples remained for downstream analysis.

Myeloid marker CpGs and deconvolution analysis:

Whole genome bisulphite sequencing (WGBS) data for Blueprint methylomes (2016 release)(23) were accessed through the RnBeads methylome resource (https://rnbeads.org/methylomes.html). Samples representing the myeloid cell compartment (venous blood monocytes and macrophage subsets) and derived from donors of age comparable to our study population (i.e. >50 years) were selected (n=13, Table S4). EPIC array and WGBS data were merged resulting in n=298,945 CpGs across each n=44 CD206+ and n=13 reference methylomes. The top 500 most variable CpGs were then used to identify ‘myeloid-marker CpGs’ and subsequently

AJRCCM Articles in Press. Published July 19, 2021 as 10.1164/rccm.202101-0004OC

deconvolute and predict myeloid cell composition of AMs using the Houseman method (71).

Differential methylation:

DMP identification was performed using the meffil R pipeline(72) which implements Epigenome-wide Association Study (EWAS) analysis. After covariate adjustment, quantile-quantile (QQ) plots were generated and inspected for EWAS QC and p-value inflation. A robust genome-wide significance threshold of P value < $9x10^{-8}$ as detailed by Mansell et al.(31) was employed to identify significant DMPs. DMRs were identified using DMRcate(35) after co variate adjustment as outlined above. IPF DMRs contained >3 CpGs ranked based on min-smoothed false discovery rate (FDR P<0.05).

Genomic and epigenomic feature enrichment:

Genomic feature distribution and annotation were identified using HOMER(73). Enrichment across epigenomic features from referenence monocytes and macrophages (Blueprint consortia) were conducted with eForge 2.0(74) and EpiAnnotator(75). Additional H3K4me1 ChIP-Seq and DNase-Seq data was accessed through the International Human Epigenomics Consortium portal (https://epigenomesportal.ca/ihec/grid.html) and ChIP-Atlas(76) respectively. HOMER was used to conduct motif enrichment in DMRs.

3D chromosomal interactions:

Promoter capture Hi-C (pcHiC)(33) was used to investigate relationships between differential DNAm and 3D chromosomal architecture. pcHi-C data was overlapped with DMPs and DMRs using bedtools and unique ‘baits’ of ‘other ends’ (OE’s)

AJRCCM Articles in Press. Published July 19, 2021 as 10.1164/rccm.202101-0004OC

overlapping DMPs and DMRs with interactions >5 in monocytes and macrophages where subsequently used to identify genes linked in 3D to differential DNAm.

Functional enrichment:

Gene ontology processes and KEGG pathway enrichment of DMR-associated genes was conducted using *goregion* function implemented in DMRcate. Additional protein-protein interaction networks were identified using NetworkAnalyst 3.0(77).

Epigenetic clock analysis:

The minfi R package(78) was used to normalize and extract EPIC array data and was submitted for Advanced Analysis utilising the DNAm age calculator (https://dnamage.genetics.ucla.edu)(79). Age-adjusted epigenetic age acceleration across the major blood cell-type-derived Hannum(80) and pan tissue-Horvath(79) clocks was calculated for each donor (n=44 total) and subsequently compared between IPF and healthy donors and myeloid cell composition.

IPF scRNA-Seq and other published datasets.

We accessed IPF lung scRNA-Seq (GSE136861) (5) using BBrowser (81). Additional UMAP projections of gene expression across immune cell types were generated via the IPF Cell Atlas (www.ipfcellatlas.com) and the corresponding Kaminski/Rosas dataset utilized. Bulk RNA-Seq and additional WGBS data from macrophage subtypes was accessed via the Blueprint data analysis portal(82).

Quantitative real-time PCR (qPCR):

Gene expression was performed as outlined previously(20, 21). Taqman probes used in this study were purchased from Thermo scientific: *LPCAT1* (Hs00227357_m1),

AJRCCM Articles in Press. Published July 19, 2021 as 10.1164/rccm.202101-0004OC

SLC12A7 (Hs00986431_m1), *SLC6A3* (Hs00997374_m1), *ARID5B* (Hs01382781_m1), *PFKFB3* (Hs00998698_m1) and *LPCAT2* (Hs01044164_m1).

Statistical analysis:

Differences in donor data were determined by Mann-Whitey or Chi-square Test for quantitative and categorical data respectively. Enrichment of overlap between DMPs/DMRs and pcHi-C data was determined using Chi-square test with Yates correction. P values for epigenetic clock residuals, qPCR and RNA-Seq data were determined via Mann-Whitney Test. Finally, spearman rank was used to identify correlations between differential DNAm, clinical variables and gene expression. All analysis was carried out using GraphPad Prism v.8.4.2

Data availability:

All EPIC methylation array data has been deposited on Gene Expression Omnibus (GSE159655).

AJRCCM Articles in Press. Published July 19, 2021 as 10.1164/rccm.202101-0004OC

	Healthy	IPF	P. value
Numbers	14	30	
Median age, year (min-max)	50 (22-67)	68 (52-82)	<0.0001
Male sex, n (%)	7 (50)	19 (63.3)	0.40
Smoking, n (%)			
- Current	1 (7.1)	0 (0)	0.57
- Ex	3 (21.4)	17 (56.6)	0.02
- Never	10 (71.4)	13 (43.3)	0.02
- Pack year history*	3.6 (0.0-20.0)	14.7 (0.0-45.0)	0.02
FACS enrichment, n (%)	7 (50)	21 (70)	0.19
FEV1*	3.2 (2.4-4.2)	2.2 (1.2-3.8)	<0.0001
FEV1 % predicted*	97.9 (80.1-114.4)	87.8 (48.0-123.5)	0.10
FVC*	4.0 (3.0-5.0)	2.7 (1.4-4.4)	<0.0001
FVC % predicted*	98.6 (78.7-114.7)	84.1 (45.7-124.9)	0.01
FEV1/FVC %*	80.2 (70.0-94.0)	82.2 (71.2-99.0)	0.23
DLCO*	107.0 (107.0-107.0)	51.2 (71.2-99)	<0.0001

Table 1: Study donor demographic data.
* mean (min-max), FEV1 -Forced expiratory volume in one second, FVC - Forced vital capacity, DLCO - Diffusing capacity for carbon monoxide.

AJRCCM Articles in Press. Published July 19, 2021 as 10.1164/rccm.202101-0004OC

Figures 1:

(A) Outline of approach to investigate relationship between airway macrophages (AMs) and other myeloid cell-types (i.e. monocytes and macrophages) DNA methylation (DNAm) as determined by EPIC and whole genome bisulphite sequencing (WGBS) respectively. Cell-type depictions were generated using www.biorender.com.

(B) Genomic feature distribution for merged AMs and myeloid cell DNAm datasets and the n=500 myeloid marker CpGs to be used in deconvolution analysis.

(C-D) Enrichment of myeloid marker CpGs across histone modifications and DNAse hypersensitivity sites (DHS) identified in myeloid cells.

(E) Gene ontology processes and KEGG pathway enrichment analysis for myeloid marker CpGs.

(F) Distribution of myeloid marker CpGs per gene.

(G) Genome track depicting epigenomic features (H3K4me1 ChIP-Seq, DHS - Blueprint) of myeloid cells across the *ARID5B* loci. The location of n=6 myeloid marker CpGs that cluster at the *ARID5B* variant 2 transcription start site (TSS) is highlighted in red and magnified further below to show DNAm profiles (beta values) across each myeloid cell type and AMs. Lines indicate average DNAm across all of the CpGs assayed in the magnified region.

Figure 2:

(A) Heatmap depicting predicted myeloid cell composition of airway macrophages (AMs - columns) after deconvolution of DNA methylation (DNAm) profiles with myeloid

AJRCCM Articles in Press. Published July 19, 2021 as 10.1164/rccm.202101-0004OC

maker-CpGs generated from reference monocyte and macrophage methylomes (rows).

(B) Difference in myeloid cell composition were evident for AMs derived from healthy and IPF donors for ‘classical’ and ‘M1 macrophages’ respectively. P-values determined by one-way ANOVA with Tukey’s correction for multiple testing.

(C) Spearman-rank correlation between donor age and composition of AMs DNAm attributed to classical monocytes and M1 macrophages.

(D) Epigenetic clock analysis indicating a correlation between chronological and epigenetic age as determined by the Hannum et. al ‘clock’ (top). By comparing residuals from two age-adjusted epigenetic ‘clocks’ (Hannum and Horvath) it was determined IPF AMs exhibited no epigenetic age acceleration compared to AMs from healthy controls.

(E) Spearman-rank correlation between epigenetic age acceleration and composition of AMs DNAm attributed to classical monocytes and M1 macrophages.

Figure 3:

(A) Quantile-quantile plots depicting the impact of adjustment for myeloid cell composition in addition to other study covariates on identification of differentially methylated positions (DMPs) in IPF. Those DMPs reaching the epigenome-wide significance (EWAS) threshold of $P<9x10^{-8}$ are highlighted in red.

(B) Volcano plot depicting impact of myeloid cell-adjustment and direction of DNA methylation (DNAm) changes of DMPs in IPF. Dashed line represents EWAS P-value threshold.

AJRCCM Articles in Press. Published July 19, 2021 as 10.1164/rccm.202101-0004OC

(C) Genome track depicting epigenomic features (H3K4me1 ChIP-Seq, DNase-I hypersensitivity - DHS - Blueprint) of myeloid cells across the *LPCAT1* loci. Regions interacting with the *LPCAT1* promoter in 3D as determined by promoter-capture HiC (pcHiC) are indicated in grey. Interactions with frequency threshold >5 in myeloid cells are highlighted in purple. The location of n=3 intronic IPF DMPs are highlighted in red and magnified further below to show methylation profiles (beta values) of healthy and IPF AMs across the respective CpGs (*). Lines indicate average methylation across all of the CpGs assayed in the magnified region.

(D) Relationship between DNAm of IPF DMPs and gene expression for *LPCAT1* across Healthy (blue) and IPF (red) donor AMs.

(E-F) Relationship between gene expression (E), methylation of an IPF-associated DMP (F) for *LPCAT1* and forced vital capacity (FVC).

Figure 4:

(A) Volcano plot depicting impact of myeloid cell-adjustment and direction of DNA methylation (DNAm) changes of differentially methylated regions (DMRs) in IPF.

(B) Genomic feature distribution for all EPIC array CpGs and those encompassed by IPF DMRs.

(C-D) Enrichment of IPF DMRs across histone modifications and DNAse-I hypersensitivity sites (DHS) in monocytes and macrophages.

(E) DNA motif enrichment in IPF DMRs.

AJRCCM Articles in Press. Published July 19, 2021 as 10.1164/rccm.202101-0004OC

Figure 5:

(A) Network depicting protein-protein interactions of DMRs-associated genes.

(B) Gene ontology processes and KEGG pathway enrichment analysis for DMR-associated genes gaining or losing DNA methylation (DNAm) in IPF.

(C) Genome track depicting epigenomic features (H3K4me1 ChIP-Seq, DNase hypersensitivity - DHS - Blueprint) of myeloid cells across the *PFKFB3* loci. The location of the IPF DMR is highlighted in red and magnified further below to show methylation profiles (beta values) at the associated n=3 CpGs (*) across healthy and IPF AMs. Lines indicate average methylation across all of the CpGs assayed in the magnified region.

(D) Relationship between DNAm of IPF DMPs and gene expression for *PFKFB3* across Healthy (blue) and IPF (red) donor AMs.

(E-F) Relationship between gene expression (E), methylation of DMR-associated CpG (F) for *PFKFB3* and forced vital capacity (FVC).

AJRCCM Articles in Press. Published July 19, 2021 as 10.1164/rccm.202101-0004OC

References

1. Byrne AJ, Maher TM, Lloyd CM. Pulmonary Macrophages: A New Therapeutic Pathway in Fibrosing Lung Disease? *Trends in Molecular Medicine* 2016; 22: 303-316.

2. Misharin AV, Morales-Nebreda L, Reyfman PA, Cuda CM, Walter JM, McQuattie-Pimentel AC, Chen CI, Anekalla KR, Joshi N, Williams KJN, Abdala-Valencia H, Yacoub TJ, Chi M, Chiu S, Gonzalez-Gonzalez FJ, Gates K, Lam AP, Nicholson TT, Homan PJ, Soberanes S, Dominguez S, Morgan VK, Saber R, Shaffer A, Hinchcliff M, Marshall SA, Bharat A, Berdnikovs S, Bhorade SM, Bartom ET, Morimoto RI, Balch WE, Sznajder JI, Chandel NS, Mutlu GM, Jain M, Gottardi CJ, Singer BD, Ridge KM, Bagheri N, Shilatifard A, Budinger GRS, Perlman H. Monocyte-derived alveolar macrophages drive lung fibrosis and persist in the lung over the life span. *J Exp Med* 2017; 214: 2387-2404.

3. Byrne AJ, Powell JE, O'Sullivan BJ, Ogger PP, Hoffland A, Cook J, Bonner KL, Hewitt RJ, Wolf S, Ghai P, Walker SA, Lukowski SW, Molyneaux PL, Saglani S, Chambers DC, Maher TM, Lloyd CM. Dynamics of human monocytes and airway macrophages during healthy aging and after transplant. *The Journal of Experimental Medicine* 2020; 217.

4. Lavin Y, Winter D, Blecher-Gonen R, David E, Keren-Shaul H, Merad M, Jung S, Amit I. Tissue-Resident Macrophage Enhancer Landscapes Are Shaped by the Local Microenvironment. *Cell* 2014; 159: 1312-1326.

5. Adams TS, Schupp JC, Poli S, Ayaub EA, Neumark N, Ahangari F, Chu SG, Raby BA, Deluliis G, Januszyk M, Duan Q, Arnett HA, Siddiqui A, Washko GR,

AJRCCM Articles in Press. Published July 19, 2021 as 10.1164/rccm.202101-0004OC

Homer R, Yan X, Rosas IO, Kaminski N. Single-cell RNA-seq reveals ectopic and aberrant lung-resident cell populations in idiopathic pulmonary fibrosis. *Science Advances* 2020; 6: eaba1983.

6. Habermann AC, Gutierrez AJ, Bui LT, Yahn SL, Winters NI, Calvi CL, Peter L, Chung M-I, Taylor CJ, Jetter C, Raju L, Roberson J, Ding G, Wood L, Sucre JMS, Richmond BW, Serezani AP, McDonnell WJ, Mallal SB, Bacchetta MJ, Loyd JE, Shaver CM, Ware LB, Bremner R, Walia R, Blackwell TS, Banovich NE, Kropski JA. Single-cell RNA sequencing reveals profibrotic roles of distinct epithelial and mesenchymal lineages in pulmonary fibrosis. *Science Advances* 2020; 6: eaba1972.

7. Reyfman PA, Walter JM, Joshi N, Anekalla KR, McQuattie-Pimentel AC, Chiu S, Fernandez R, Akbarpour M, Chen C-I, Ren Z, Verma R, Abdala-Valencia H, Nam K, Chi M, Han S, Gonzalez-Gonzalez FJ, Soberanes S, Watanabe S, Williams KJN, Flozak AS, Nicholson TT, Morgan VK, Winter DR, Hinchcliff M, Hrusch CL, Guzy RD, Bonham CA, Sperling AI, Bag R, Hamanaka RB, Mutlu GM, Yeldandi AV, Marshall SA, Shilatifard A, Amaral LAN, Perlman H, Sznajder JI, Argento AC, Gillespie CT, Dematte J, Jain M, Singer BD, Ridge KM, Lam AP, Bharat A, Bhorade SM, Gottardi CJ, Budinger GRS, Misharin AV. Single-Cell Transcriptomic Analysis of Human Lung Provides Insights into the Pathobiology of Pulmonary Fibrosis. *American Journal of Respiratory and Critical Care Medicine* 2018; 199: 1517-1536.

8. Wallner S, Schröder C, Leitão E, Berulava T, Haak C, Beißer D, Rahmann S, Richter AS, Manke T, Bönisch U, Arrigoni L, Fröhler S, Klironomos F, Chen W, Rajewsky N, Müller F, Ebert P, Lengauer T, Barann M, Rosenstiel P,

AJRCCM Articles in Press. Published July 19, 2021 as 10.1164/rccm.202101-0004OC

Gasparoni G, Nordström K, Walter J, Brors B, Zipprich G, Felder B, Klein-Hitpass L, Attenberger C, Schmitz G, Horsthemke B. Epigenetic dynamics of monocyte-to-macrophage differentiation. *Epigenetics & Chromatin* 2016; 9: 33.

9. Tirado-Magallanes R, Rebbani K, Lim R, Pradhan S, Benoukraf T. Whole genome DNA methylation: beyond genes silencing. *Oncotarget* 2017; 8: 5629-5637.

10. Schübeler D. Function and information content of DNA methylation. *Nature* 2015; 517: 321-326.

11. Chen Y, Armstrong DA, Salas LA, Hazlett HF, Nymon AB, Dessaint JA, Aridgides DS, Mellinger DL, Liu X, Christensen BC, Ashare A. Genome-wide DNA methylation profiling shows a distinct epigenetic signature associated with lung macrophages in cystic fibrosis. *Clinical epigenetics* 2018; 10: 152-152.

12. Fricker M, Gibson PG. Macrophage dysfunction in the pathogenesis and treatment of asthma. *European Respiratory Journal* 2017; 50: 1700196.

13. He L-X, Tang Z-H, Huang Q-S, Li W-H. DNA Methylation: A Potential Biomarker of Chronic Obstructive Pulmonary Disease. *Frontiers in cell and developmental biology* 2020; 8: 585-585.

14. Armstrong DA, Chen Y, Dessaint JA, Aridgides DS, Channon JY, Mellinger DL, Christensen BC, Ashare A. DNA Methylation Changes in Regional Lung Macrophages Are Associated with Metabolic Differences. *ImmunoHorizons* 2019; 3: 274.

AJRCCM Articles in Press. Published July 19, 2021 as 10.1164/rccm.202101-0004OC

15. Martinez FJ, Collard HR, Pardo A, Raghu G, Richeldi L, Selman M, Swigris JJ, Taniguchi H, Wells AU. Idiopathic pulmonary fibrosis. *Nature Reviews Disease Primers* 2017; 3: 17074.

16. Chambers RC, Mercer PF. Mechanisms of alveolar epithelial injury, repair, and fibrosis. *Annals of the American Thoracic Society* 2015; 12 Suppl 1: S16-S20.

17. Allen RJ, Guillen-Guio B, Oldham JM, Ma SF, Dressen A, Paynton ML, Kraven LM, Obeidat M, Li X, Ng M, Braybrooke R, Molina-Molina M, Hobbs BD, Putman RK, Sakornsakolpat P, Booth HL, Fahy WA, Hart SP, Hill MR, Hirani N, Hubbard RB, McAnulty RJ, Millar AB, Navaratnam V, Oballa E, Parfrey H, Saini G, Whyte MKB, Zhang Y, Kaminski N, Adegunsoye A, Strek ME, Neighbors M, Sheng XR, Gudmundsson G, Gudnason V, Hatabu H, Lederer DJ, Manichaikul A, Newell JD, Jr., O'Connor GT, Ortega VE, Xu H, Fingerlin TE, Bossé Y, Hao K, Joubert P, Nickle DC, Sin DD, Timens W, Furniss D, Morris AP, Zondervan KT, Hall IP, Sayers I, Tobin MD, Maher TM, Cho MH, Hunninghake GM, Schwartz DA, Yaspan BL, Molyneaux PL, Flores C, Noth I, Jenkins RG, Wain LV. Genome-Wide Association Study of Susceptibility to Idiopathic Pulmonary Fibrosis. *Am J Respir Crit Care Med* 2020; 201: 564-574.

18. Molyneaux PL, Willis-Owen SAG, Cox MJ, James P, Cowman S, Loebinger M, Blanchard A, Edwards LM, Stock C, Daccord C, Renzoni EA, Wells AU, Moffatt MF, Cookson WOC, Maher TM. Host–Microbial Interactions in Idiopathic Pulmonary Fibrosis. *American Journal of Respiratory and Critical Care Medicine* 2017; 195: 1640-1650.

AJRCCM Articles in Press. Published July 19, 2021 as 10.1164/rccm.202101-0004OC

19. Vancheri C, Failla M, Crimi N, Raghu G. Idiopathic pulmonary fibrosis: a disease with similarities and links to cancer biology. *European Respiratory Journal* 2010; 35: 496.

20. Allden SJ, Ogger PP, Ghai P, McErlean P, Hewitt R, Toshner R, Walker SA, Saunders P, Kingston S, Molyneaux PL, Maher TM, Lloyd CM, Byrne AJ. The Transferrin Receptor CD71 Delineates Functionally Distinct Airway Macrophage Subsets during Idiopathic Pulmonary Fibrosis. *American Journal of Respiratory and Critical Care Medicine* 2019; 200: 209-219.

21. Ogger PP, Albers GJ, Hewitt RJ, O'Sullivan BJ, Powell JE, Calamita E, Ghai P, Walker SA, McErlean P, Saunders P, Kingston S, Molyneaux PL, Halket JM, Gray R, Chambers DC, Maher TM, Lloyd CM, Byrne AJ. Itaconate controls the severity of pulmonary fibrosis. *Science Immunology* 2020; 5: eabc1884.

22. Pidsley R, Zotenko E, Peters TJ, Lawrence MG, Risbridger GP, Molloy P, Van Djik S, Muhlhausler B, Stirzaker C, Clark SJ. Critical evaluation of the Illumina MethylationEPIC BeadChip microarray for whole-genome DNA methylation profiling. *Genome Biol* 2016; 17: 208.

23. Stunnenberg HG, Hirst M. The International Human Epigenome Consortium: A Blueprint for Scientific Collaboration and Discovery. *Cell* 2016; 167: 1145-1149.

24. Okazaki Y, Murray J, Ehsani A, Clark J, Whitson RH, Hirose L, Yanaka N, Itakura K. Increased glucose metabolism in Arid5b−/− skeletal muscle is associated with the down-regulation of TBC1 domain family member 1 (TBC1D1). *Biological Research* 2020; 53: 45.

AJRCCM Articles in Press. Published July 19, 2021 as 10.1164/rccm.202101-0004OC

25. Horvath S, Raj K. DNA methylation-based biomarkers and the epigenetic clock theory of ageing. *Nature Reviews Genetics* 2018; 19: 371-384.

26. Horvath S, Levine AJ. HIV-1 Infection Accelerates Age According to the Epigenetic Clock. *J Infect Dis* 2015; 212: 1563-1573.

27. Horvath S, Ritz BR. Increased epigenetic age and granulocyte counts in the blood of Parkinson's disease patients. *Aging (Albany NY)* 2015; 7: 1130-1142.

28. Horvath S, Garagnani P, Bacalini MG, Pirazzini C, Salvioli S, Gentilini D, Di Blasio AM, Giuliani C, Tung S, Vinters HV, Franceschi C. Accelerated epigenetic aging in Down syndrome. *Aging Cell* 2015; 14: 491-495.

29. Marioni RE, Shah S, McRae AF, Chen BH, Colicino E, Harris SE, Gibson J, Henders AK, Redmond P, Cox SR, Pattie A, Corley J, Murphy L, Martin NG, Montgomery GW, Feinberg AP, Fallin MD, Multhaup ML, Jaffe AE, Joehanes R, Schwartz J, Just AC, Lunetta KL, Murabito JM, Starr JM, Horvath S, Baccarelli AA, Levy D, Visscher PM, Wray NR, Deary IJ. DNA methylation age of blood predicts all-cause mortality in later life. *Genome Biol* 2015; 16: 25.

30. El Khoury LY, Gorrie-Stone T, Smart M, Hughes A, Bao Y, Andrayas A, Burrage J, Hannon E, Kumari M, Mill J, Schalkwyk LC. Systematic underestimation of the epigenetic clock and age acceleration in older subjects. *Genome Biol* 2019; 20: 283.

31. Mansell G, Gorrie-Stone TJ, Bao Y, Kumari M, Schalkwyk LS, Mill J, Hannon E. Guidance for DNA methylation studies: statistical insights from the Illumina EPIC array. *BMC Genomics* 2019; 20: 366.

AJRCCM Articles in Press. Published July 19, 2021 as 10.1164/rccm.202101-0004OC

32. Du Y, Wang Q, Zhang X, Wang X, Qin C, Sheng Z, Yin H, Jiang C, Li J, Xu T. Lysophosphatidylcholine acyltransferase 1 upregulation and concomitant phospholipid alterations in clear cell renal cell carcinoma. *J Exp Clin Cancer Res* 2017; 36: 66.

33. Javierre BM, Burren OS, Wilder SP, Kreuzhuber R, Hill SM, Sewitz S, Cairns J, Wingett SW, Varnai C, Thiecke MJ, Burden F, Farrow S, Cutler AJ, Rehnstrom K, Downes K, Grassi L, Kostadima M, Freire-Pritchett P, Wang F, Stunnenberg HG, Todd JA, Zerbino DR, Stegle O, Ouwehand WH, Frontini M, Wallace C, Spivakov M, Fraser P. Lineage-Specific Genome Architecture Links Enhancers and Non-coding Disease Variants to Target Gene Promoters. *Cell* 2016; 167: 1369-1384.e1319.

34. Richeldi L, Ryerson CJ, Lee JS, Wolters PJ, Koth LL, Ley B, Elicker BM, Jones KD, King TE, Ryu JH, Collard HR. Relative versus absolute change in forced vital capacity in idiopathic pulmonary fibrosis. *Thorax* 2012; 67: 407.

35. Peters TJ, Buckley MJ, Statham AL, Pidsley R, Samaras K, V Lord R, Clark SJ, Molloy PL. De novo identification of differentially methylated regions in the human genome. *Epigenetics Chromatin* 2015; 8: 6.

36. Finucane OM, Sugrue J, Rubio-Araiz A, Guillot-Sestier MV, Lynch MA. The NLRP3 inflammasome modulates glycolysis by increasing PFKFB3 in an IL-1β-dependent manner in macrophages. *Sci Rep* 2019; 9: 4034.

37. Herazo-Maya JD, Sun J, Molyneaux PL, Li Q, Villalba JA, Tzouvelekis A, Lynn H, Juan-Guardela BM, Risquez C, Osorio JC, Yan X, Michel G, Aurelien N, Lindell KO, Klesen MJ, Moffatt MF, Cookson WO, Zhang Y, Garcia JGN, Noth

AJRCCM Articles in Press. Published July 19, 2021 as 10.1164/rccm.202101-0004OC

I, Prasse A, Bar-Joseph Z, Gibson KF, Zhao H, Herzog EL, Rosas IO, Maher TM, Kaminski N. Validation of a 52-gene risk profile for outcome prediction in patients with idiopathic pulmonary fibrosis: an international, multicentre, cohort study. *The Lancet Respiratory Medicine* 2017; 5: 857-868.

38. Herazo-Maya JD, Noth I, Duncan SR, Kim S, Ma S-F, Tseng GC, Feingold E, Juan-Guardela BM, Richards TJ, Lussier Y, Huang Y, Vij R, Lindell KO, Xue J, Gibson KF, Shapiro SD, Garcia JGN, Kaminski N. Peripheral Blood Mononuclear Cell Gene Expression Profiles Predict Poor Outcome in Idiopathic Pulmonary Fibrosis. *Science Translational Medicine* 2013; 5: 205ra136.

39. Scott MKD, Quinn K, Li Q, Carroll R, Warsinske H, Vallania F, Chen S, Carns MA, Aren K, Sun J, Koloms K, Lee J, Baral J, Kropski J, Zhao H, Herzog E, Martinez FJ, Moore BB, Hinchcliff M, Denny J, Kaminski N, Herazo-Maya JD, Shah NH, Khatri P. Increased monocyte count as a cellular biomarker for poor outcomes in fibrotic diseases: a retrospective, multicentre cohort study. *The Lancet Respiratory Medicine* 2019; 7: 497-508.

40. Titus AJ, Gallimore RM, Salas LA, Christensen BC. Cell-type deconvolution from DNA methylation: a review of recent applications. *Human molecular genetics* 2017; 26: R216-R224.

41. Yang IV, Pedersen BS, Rabinovich E, Hennessy CE, Davidson EJ, Murphy E, Guardela BJ, Tedrow JR, Zhang Y, Singh MK, Correll M, Schwarz MI, Geraci M, Sciurba FC, Quackenbush J, Spira A, Kaminski N, Schwartz DA. Relationship of DNA Methylation and Gene Expression in Idiopathic

AJRCCM Articles in Press. Published July 19, 2021 as 10.1164/rccm.202101-0004OC

Pulmonary Fibrosis. *American Journal of Respiratory and Critical Care Medicine* 2014; 190: 1263-1272.

42. Sanders YY, Ambalavanan N, Halloran B, Zhang X, Liu H, Crossman DK, Bray M, Zhang K, Thannickal VJ, Hagood JS. Altered DNA Methylation Profile in Idiopathic Pulmonary Fibrosis. *American Journal of Respiratory and Critical Care Medicine* 2012; 186: 525-535.

43. Yang IV, Schwartz DA. Epigenetics of idiopathic pulmonary fibrosis. *Transl Res* 2015; 165: 48-60.

44. Selman M, López-Otín C, Pardo A. Age-driven developmental drift in the pathogenesis of idiopathic pulmonary fibrosis. *Eur Respir J* 2016; 48: 538-552.

45. Alder JK, Chen JJ, Lancaster L, Danoff S, Su SC, Cogan JD, Vulto I, Xie M, Qi X, Tuder RM, Phillips JA, Lansdorp PM, Loyd JE, Armanios MY. Short telomeres are a risk factor for idiopathic pulmonary fibrosis. *Proc Natl Acad Sci U S A* 2008; 105: 13051-13056.

46. Kropski JA, Pritchett JM, Zoz DF, Crossno PF, Markin C, Garnett ET, Degryse AL, Mitchell DB, Polosukhin VV, Rickman OB, Choi L, Cheng DS, McConaha ME, Jones BR, Gleaves LA, McMahon FB, Worrell JA, Solus JF, Ware LB, Lee JW, Massion PP, Zaynagetdinov R, White ES, Kurtis JD, Johnson JE, Groshong SD, Lancaster LH, Young LR, Steele MP, Phillips Iii JA, Cogan JD, Loyd JE, Lawson WE, Blackwell TS. Extensive phenotyping of individuals at risk for familial interstitial pneumonia reveals clues to the pathogenesis of interstitial lung disease. *Am J Respir Crit Care Med* 2015; 191: 417-426.

AJRCCM Articles in Press. Published July 19, 2021 as 10.1164/rccm.202101-0004OC

47. Minagawa S, Araya J, Numata T, Nojiri S, Hara H, Yumino Y, Kawaishi M, Odaka M, Morikawa T, Nishimura SL, Nakayama K, Kuwano K. Accelerated epithelial cell senescence in IPF and the inhibitory role of SIRT6 in TGF-β-induced senescence of human bronchial epithelial cells. *Am J Physiol Lung Cell Mol Physiol* 2011; 300: L391-401.

48. Disayabutr S, Kim EK, Cha SI, Green G, Naikawadi RP, Jones KD, Golden JA, Schroeder A, Matthay MA, Kukreja J, Erle DJ, Collard HR, Wolters PJ. miR-34 miRNAs Regulate Cellular Senescence in Type II Alveolar Epithelial Cells of Patients with Idiopathic Pulmonary Fibrosis. *PLoS One* 2016; 11: e0158367.

49. Bell CG, Lowe R, Adams PD, Baccarelli AA, Beck S, Bell JT, Christensen BC, Gladyshev VN, Heijmans BT, Horvath S, Ideker T, Issa J-PJ, Kelsey KT, Marioni RE, Reik W, Relton CL, Schalkwyk LC, Teschendorff AE, Wagner W, Zhang K, Rakyan VK. DNA methylation aging clocks: challenges and recommendations. *Genome Biology* 2019; 20: 249.

50. Shchukina I, Bagaitkar J, Shpynov O, Loginicheva E, Porter S, Mogilenko DA, Wolin E, Collins P, Demidov G, Artomov M, Zaitsev K, Sidorov S, Camell C, Bambouskova M, Arthur L, Swain A, Panteleeva A, Dievskii A, Kurbatsky E, Tsurinov P, Chernyatchik R, Dixit VD, Jovanovic M, Stewart SA, Daly MJ, Dmitriev S, Oltz EM, Artyomov MN. Epigenetic aging of classical monocytes from healthy individuals. *bioRxiv* 2020: 2020.2005.2010.087023.

51. Corces MR, Buenrostro JD, Wu B, Greenside PG, Chan SM, Koenig JL, Snyder MP, Pritchard JK, Kundaje A, Greenleaf WJ, Majeti R, Chang HY. Lineage-

AJRCCM Articles in Press. Published July 19, 2021 as 10.1164/rccm.202101-0004OC

specific and single-cell chromatin accessibility charts human hematopoiesis and leukemia evolution. *Nature Genetics* 2016; 48: 1193-1203.

52. Okuno Y, Inoue K, Imai Y. Novel insights into histone modifiers in adipogenesis. *Adipocyte* 2013; 2: 285-288.

53. Claussnitzer M, Dankel SN, Kim K-H, Quon G, Meuleman W, Haugen C, Glunk V, Sousa IS, Beaudry JL, Puviindran V, Abdennur NA, Liu J, Svensson P-A, Hsu Y-H, Drucker DJ, Mellgren G, Hui C-C, Hauner H, Kellis M. FTO Obesity Variant Circuitry and Adipocyte Browning in Humans. *New England Journal of Medicine* 2015; 373: 895-907.

54. Baba A, Ohtake F, Okuno Y, Yokota K, Okada M, Imai Y, Ni M, Meyer CA, Igarashi K, Kanno J, Brown M, Kato S. PKA-dependent regulation of the histone lysine demethylase complex PHF2–ARID5B. *Nature Cell Biology* 2011; 13: 668-675.

55. Cichocki F, Wu C-Y, Zhang B, Felices M, Tesi B, Tuininga K, Dougherty P, Taras E, Hinderlie P, Blazar BR, Bryceson YT, Miller JS. ARID5B regulates metabolic programming in human adaptive NK cells. *The Journal of experimental medicine* 2018; 215: 2379-2395.

56. Liu Y, Reynolds LM, Ding J, Hou L, Lohman K, Young T, Cui W, Huang Z, Grenier C, Wan M, Stunnenberg HG, Siscovick D, Hou L, Psaty BM, Rich SS, Rotter JI, Kaufman JD, Burke GL, Murphy S, Jacobs DR, Post W, Hoeschele I, Bell DA, Herrington D, Parks JS, Tracy RP, McCall CE, Stein JH. Blood monocyte transcriptome and epigenome analyses reveal loci associated with human atherosclerosis. *Nature Communications* 2017; 8: 393.

AJRCCM Articles in Press. Published July 19, 2021 as 10.1164/rccm.202101-0004OC

57. El-Chemaly S, Malide D, Yao J, Nathan SD, Rosas IO, Gahl WA, Moss J, Gochuico BR. Glucose transporter-1 distribution in fibrotic lung disease: association with [^{18}F]-2-fluoro-2-deoxyglucose-PET scan uptake, inflammation, and neovascularization. *Chest* 2013; 143: 1685-1691.

58. Tsitoura E, Vasarmidi E, Bibaki E, Trachalaki A, Koutoulaki C, Papastratigakis G, Papadogiorgaki S, Chalepakis G, Tzanakis N, Antoniou KM. Accumulation of damaged mitochondria in alveolar macrophages with reduced OXPHOS related gene expression in IPF. *Respir Res* 2019; 20: 264.

59. Leslie J, Macia MG, Luli S, Worrell JC, Reilly WJ, Paish HL, Knox A, Barksby BS, Gee LM, Zaki MYW, Collins AL, Burgoyne RA, Cameron R, Bragg C, Xu X, Chung GW, Brown CDA, Blanchard AD, Nanthakumar CB, Karsdal M, Robinson SM, Manas DM, Sen G, French J, White SA, Murphy S, Trost M, Zakrzewski JL, Klein U, Schwabe RF, Mederacke I, Nixon C, Bird T, Teuwen L-A, Schoonjans L, Carmeliet P, Mann J, Fisher AJ, Sheerin NS, Borthwick LA, Mann DA, Oakley F. c-Rel orchestrates energy-dependent epithelial and macrophage reprogramming in fibrosis. *Nature Metabolism* 2020.

60. Tawakol A, Singh P, Mojena M, Pimentel-Santillana M, Emami H, MacNabb M, Rudd JHF, Narula J, Enriquez JA, Través PG, Fernández-Velasco M, Bartrons R, Martín-Sanz P, Fayad ZA, Tejedor A, Boscá L. HIF-1α and PFKFB3 Mediate a Tight Relationship Between Proinflammatory Activation and Anerobic Metabolism in Atherosclerotic Macrophages. *Arteriosclerosis, thrombosis, and vascular biology* 2015; 35: 1463-1471.

AJRCCM Articles in Press. Published July 19, 2021 as 10.1164/rccm.202101-0004OC

61. Jiang H, Shi H, Sun M, Wang Y, Meng Q, Guo P, Cao Y, Chen J, Gao X, Li E, Liu J. PFKFB3-Driven Macrophage Glycolytic Metabolism Is a Crucial Component of Innate Antiviral Defense. *J Immunol* 2016; 197: 2880-2890.

62. Chen X, Hyatt BA, Mucenski ML, Mason RJ, Shannon JM. Identification and characterization of a lysophosphatidylcholine acyltransferase in alveolar type II cells. *Proc Natl Acad Sci U S A* 2006; 103: 11724-11729.

63. Bridges JP, Ikegami M, Brilli LL, Chen X, Mason RJ, Shannon JM. LPCAT1 regulates surfactant phospholipid synthesis and is required for transitioning to air breathing in mice. *The Journal of Clinical Investigation* 2010; 120: 1736-1748.

64. Bi J, Ichu T-A, Zanca C, Yang H, Zhang W, Gu Y, Chowdhry S, Reed A, Ikegami S, Turner KM, Zhang W, Villa GR, Wu S, Quehenberger O, Yong WH, Kornblum HI, Rich JN, Cloughesy TF, Cavenee WK, Furnari FB, Cravatt BF, Mischel PS. Oncogene Amplification in Growth Factor Signaling Pathways Renders Cancers Dependent on Membrane Lipid Remodeling. *Cell Metabolism* 2019; 30: 525-538.e528.

65. Xu Y, Mizuno T, Sridharan A, Du Y, Guo M, Tang J, Wikenheiser-Brokamp KA, Perl A-KT, Funari VA, Gokey JJ, Stripp BR, Whitsett JA. Single-cell RNA sequencing identifies diverse roles of epithelial cells in idiopathic pulmonary fibrosis. *JCI Insight* 2017; 1.

66. Suryadevara V, Ramchandran R, Kamp DW, Natarajan V. Lipid Mediators Regulate Pulmonary Fibrosis: Potential Mechanisms and Signaling Pathways. *International Journal of Molecular Sciences* 2020; 21.

AJRCCM Articles in Press. Published July 19, 2021 as 10.1164/rccm.202101-0004OC

67. Lavender P, Kelly A, Hendy E, McErlean P. CRISPR-based reagents to study the influence of the epigenome on gene expression. *Clinical & Experimental Immunology* 2018; 194: 9-16.

68. Qu J, Zhu L, Zhou Z, Chen P, Liu S, Locy ML, Thannickal VJ, Zhou Y. Reversing Mechanoinductive DSP Expression by CRISPR/dCas9–mediated Epigenome Editing. *American Journal of Respiratory and Critical Care Medicine* 2018; 198: 599-609.

69. Müller F, Scherer M, Assenov Y, Lutsik P, Walter J, Lengauer T, Bock C. RnBeads 2.0: comprehensive analysis of DNA methylation data. *Genome Biol* 2019; 20: 55.

70. Pidsley R, Y Wong CC, Volta M, Lunnon K, Mill J, Schalkwyk LC. A data-driven approach to preprocessing Illumina 450K methylation array data. *BMC Genomics* 2013; 14: 293.

71. Houseman EA, Kile ML, Christiani DC, Ince TA, Kelsey KT, Marsit CJ. Reference-free deconvolution of DNA methylation data and mediation by cell composition effects. *BMC Bioinformatics* 2016; 17: 259.

72. Min JL, Hemani G, Davey Smith G, Relton C, Suderman M. Meffil: efficient normalization and analysis of very large DNA methylation datasets. *Bioinformatics* 2018; 34: 3983-3989.

73. Heinz S, Benner C, Spann N, Bertolino E, Lin YC, Laslo P, Cheng JX, Murre C, Singh H, Glass CK. Simple combinations of lineage-determining transcription factors prime cis-regulatory elements required for macrophage and B cell identities. *Mol Cell* 2010; 38: 576-589.

AJRCCM Articles in Press. Published July 19, 2021 as 10.1164/rccm.202101-0004OC

74. Breeze CE, Reynolds AP, van Dongen J, Dunham I, Lazar J, Neph S, Vierstra J, Bourque G, Teschendorff AE, Stamatoyannopoulos JA, Beck S. eFORGE v2.0: updated analysis of cell type-specific signal in epigenomic data. *Bioinformatics* 2019; 35: 4767-4769.

75. Pageaud Y, Plass C, Assenov Y. Enrichment analysis with EpiAnnotator. *Bioinformatics* 2018; 34: 1781-1783.

76. Oki S, Ohta T, Shioi G, Hatanaka H, Ogasawara O, Okuda Y, Kawaji H, Nakaki R, Sese J, Meno C. ChIP-Atlas: a data-mining suite powered by full integration of public ChIP-seq data. *EMBO reports* 2018; 19: e46255.

77. Zhou G, Soufan O, Ewald J, Hancock REW, Basu N, Xia J. NetworkAnalyst 3.0: a visual analytics platform for comprehensive gene expression profiling and meta-analysis. *Nucleic Acids Res* 2019; 47: W234-W241.

78. Aryee MJ, Jaffe AE, Corrada-Bravo H, Ladd-Acosta C, Feinberg AP, Hansen KD, Irizarry RA. Minfi: a flexible and comprehensive Bioconductor package for the analysis of Infinium DNA methylation microarrays. *Bioinformatics (Oxford, England)* 2014; 30: 1363-1369.

79. Horvath S. DNA methylation age of human tissues and cell types. *Genome Biology* 2013; 14: 3156.

80. Hannum G, Guinney J, Zhao L, Zhang L, Hughes G, Sadda S, Klotzle B, Bibikova M, Fan JB, Gao Y, Deconde R, Chen M, Rajapakse I, Friend S, Ideker T, Zhang K. Genome-wide methylation profiles reveal quantitative views of human aging rates. *Mol Cell* 2013; 49: 359-367.

AJRCCM Articles in Press. Published July 19, 2021 as 10.1164/rccm.202101-0004OC

81. Le T, Phan T, Pham M, Tran D, Lam L, Nguyen T, Truong T, Vuong H, Luu T, Phung N, Pham N, Nguyen T, Pham O, Nguyen A, Nguyen H, Tran H, Tran L, Nguyen HA, Tran T, Nguyen N, Tran N, Boysen C, Nguyen U, Pham V, Kim T, Pham N, Gill T, Pham S. BBrowser: Making single-cell data easily accessible. *bioRxiv* 2020: 2020.2012.2011.414136.

82. Fernández JM, de la Torre V, Richardson D, Royo R, Puiggròs M, Moncunill V, Fragkogianni S, Clarke L, Flicek P, Rico D, Torrents D, Carrillo de Santa Pau E, Valencia A. The BLUEPRINT Data Analysis Portal. *Cell Systems* 2016; 3: 491-495.e495.

AJRCCM Articles in Press. Published July 19, 2021 as 10.1164/rccm.202101-0004OC

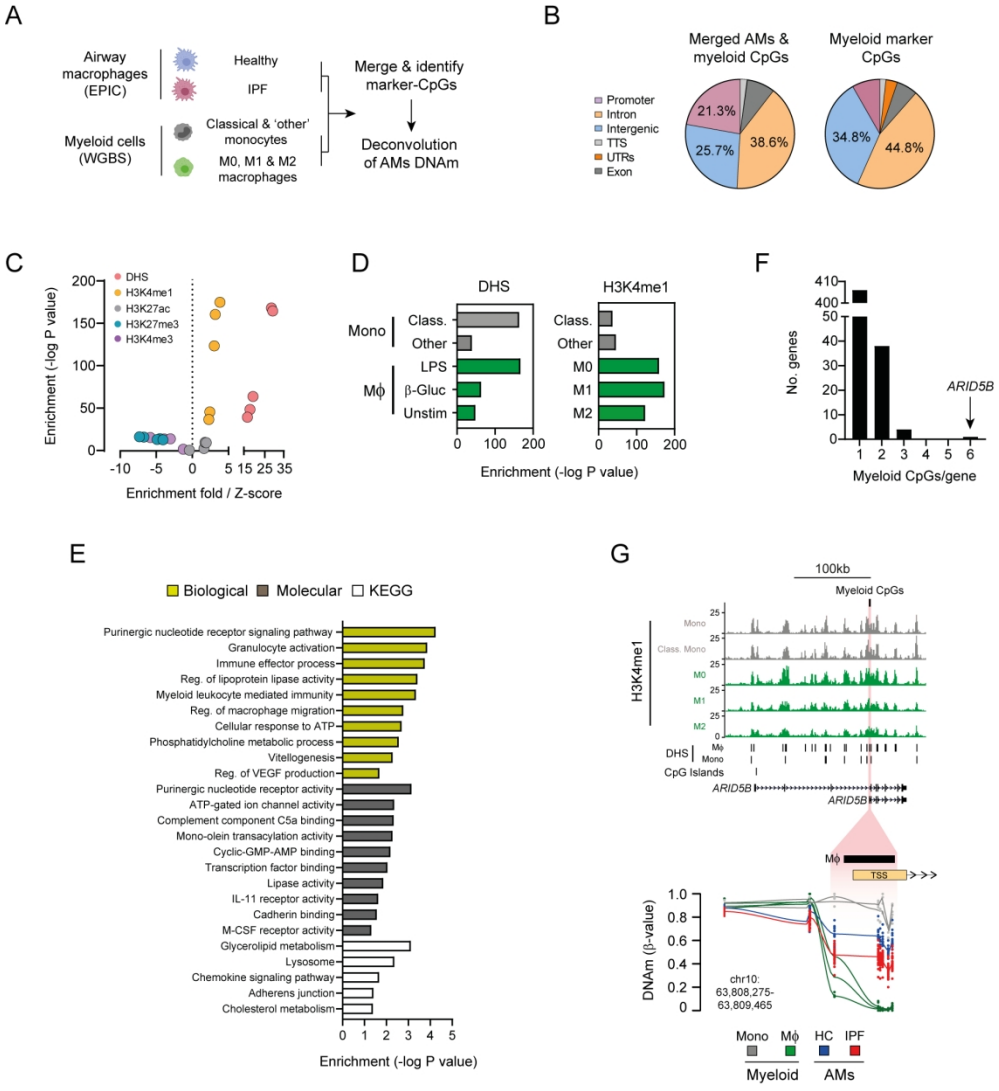

Figure 1

AJRCCM Articles in Press. Published July 19, 2021 as 10.1164/rccm.202101-0004OC

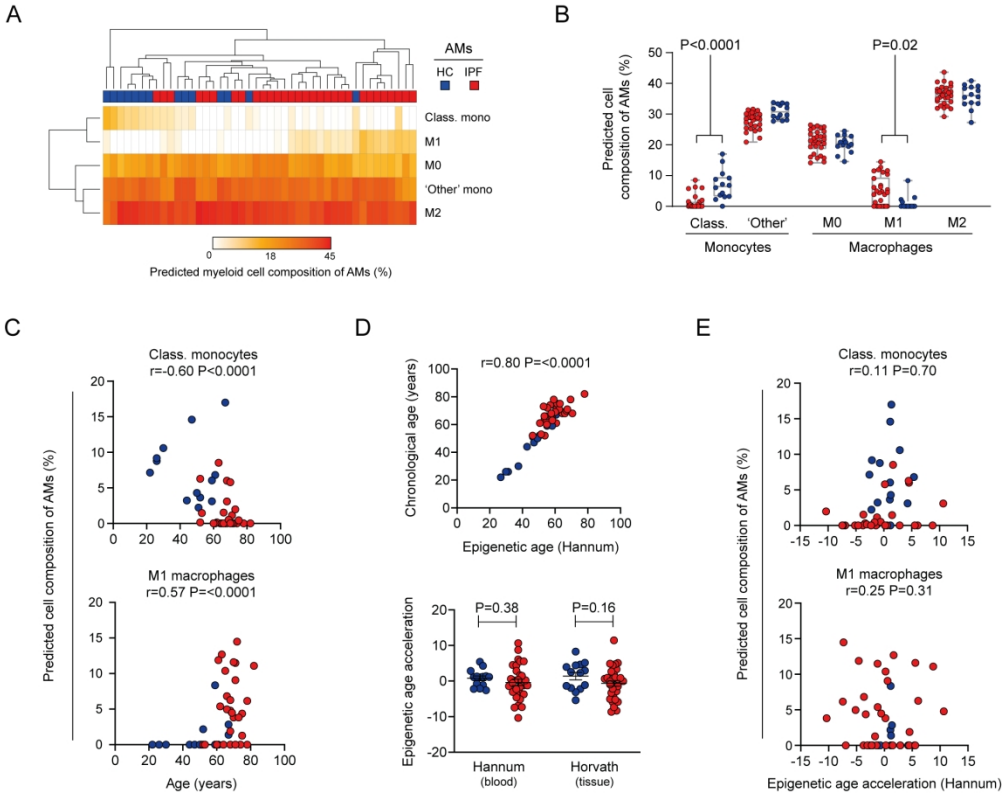

Figure 2

AJRCCM Articles in Press. Published July 19, 2021 as 10.1164/rccm.202101-0004OC

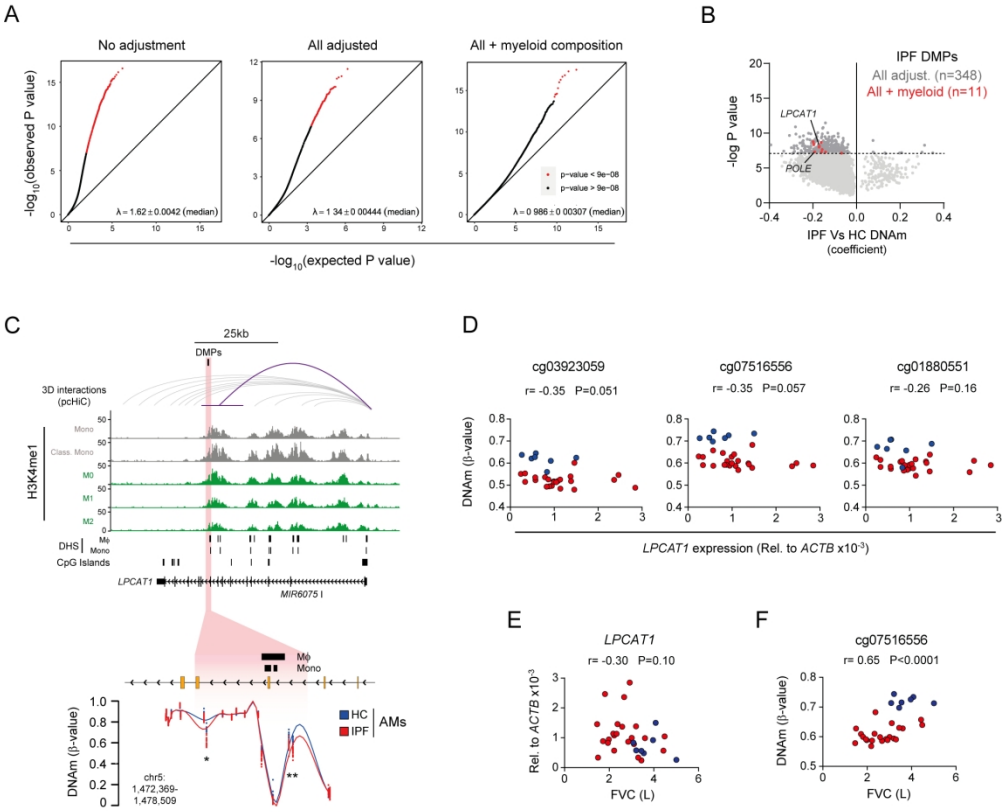

Figure 3

AJRCCM Articles in Press. Published July 19, 2021 as 10.1164/rccm.202101-0004OC

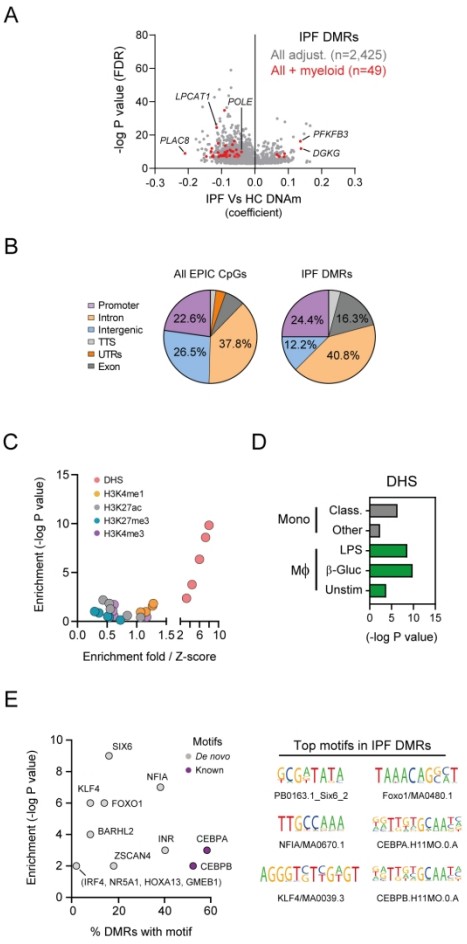

Figure 4

AJRCCM Articles in Press. Published July 19, 2021 as 10.1164/rccm.202101-0004OC

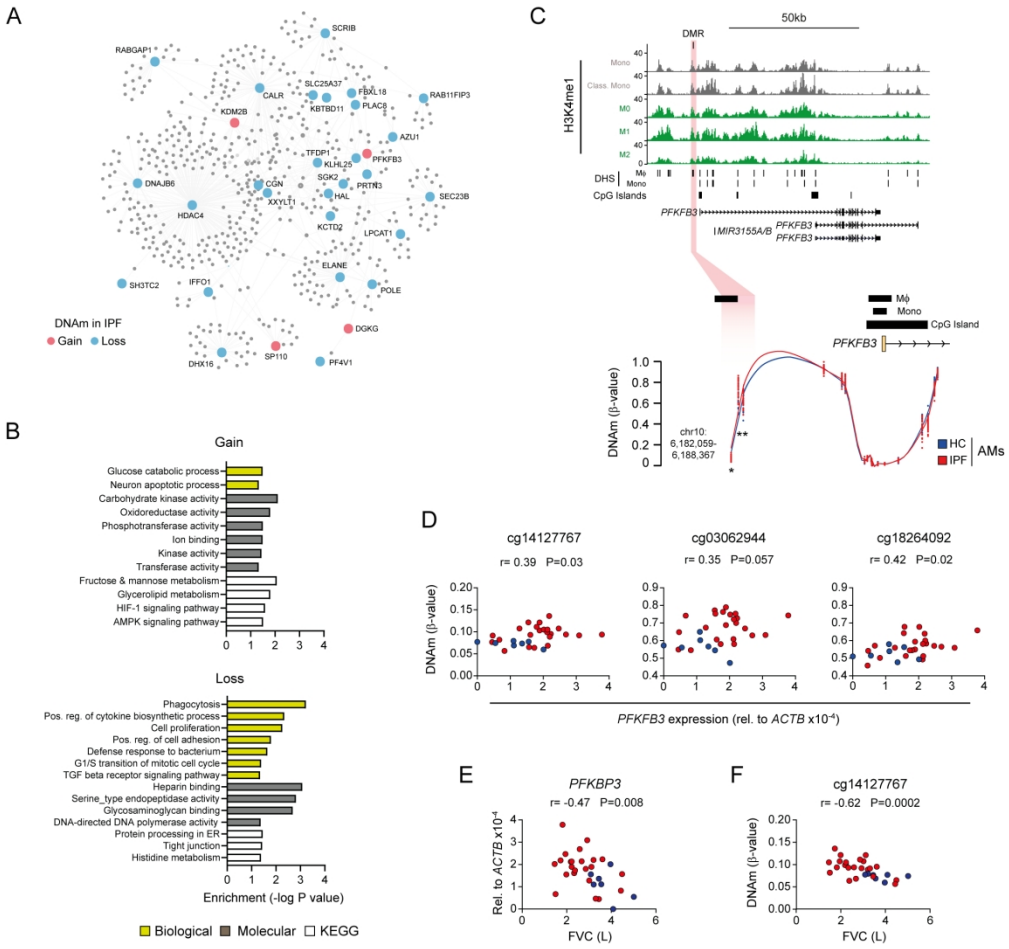

Figure 5

AJRCCM Articles in Press. Published July 19, 2021 as 10.1164/rccm.202101-0004OC

Online Data Supplement

Figure S1

(A) Disease origin and cell-type expression of *ARID5B* in single cell RNA-Seq data from the IPF lung (GSE136861). Gene expression is projected over UMAP representation of all disease/cell-types with brighter colours indicating more expression. UMAPs generated via www.ipfcellatlas.com.

(B-C) *ARID5B* gene expression in AMs from healthy and IPF donors and macrophage subsets (Blueprint consortia) as determined by qPCR and RNA-Seq respectively.

* P<0.05, ** P<0.01 Mann-Whitey Test.

(D) Heatmap depicting DNA methylation (DNAm) profiles across myeloid cells (i.e. monocytes and M0, M1, M2 macrophages) and AMs from healthy and IPF donors for genes containing >2 myeloid marker CpGs (Table S1).

(E) Spearman-rank correlations for chronological and epigenetic age as determined by the Horvath et. al 'clock'.

(F) Residuals across other epigenetic clocks less likely to be impacted by the non-linear effect of DNAm and ageing.

(G) Spearman-rank correlations for epigenetic age acceleration and composition of AMs DNAm attributed to classical monocytes (right) and M1 macrophages (left).

Figure S2

(A) PCA plot of normalized DNA methylation (DNAm) data for all CpGs prior to differential analysis indicating separation of healthy and IPF AMs.

(B) Sources of variation in DNAm dataset across the first 5 principal components for all CpGs. Associated P values were generated through RnBeads pipline.

AJRCCM Articles in Press. Published July 19, 2021 as 10.1164/rccm.202101-0004OC

(C-D) Plots depicting changes in DNAm (beta value) for healthy and IPF donors across Intronic (C) and intergenic (D) DMPs (Table S2).

(E) Enrichment of IPF differentially methylated positions (DMPs) across DNAse hypersensitivity sites (DHS) in monocytes and macrophages.

(F-G) *LPCAT1* gene expression across single cell RNA-Seq (scRNA-Seq) data from the IPF lung (refer to Figure 1B) and AMs from healthy and IPF donors as determined by qPCR.

(H) All regions interacting with the *LPCAT1* promoter in 3D as determined by promoter-capture HiC (pcHiC). In addition to self-interacting with the region containing IPF DMPs (purple, Figure 2E), *LPCAT1* additionally interacts with the promoters of *SLC6A3* and *SLC12A7*. Dashed line indicates interactions with frequency threshold >5.

(I) Relationship between DNAm of IPF DMPs and gene expression for *SLC6A3* across Healthy (blue) and IPF (red) donor AMs. No *SLC12A7* gene expression was detected in AMs.

(J) DNAm of the single CpG encompassing *LPCAT2* identified in DMP analysis with associated significance pre- and post-adjustment for AMs myeloid cell composition. No CpGs encompassing *LPCAT2* were identified in DMR analysis.

(K) *LPCAT2* gene expression in AMs from healthy and IPF donors by qPCR.

(L) Spearman-rank correlation between *LPCAT2* DNAm and gene expression.

(M) Comparison between *LPCAT1 and LPCAT2* gene expression across macrophage subtypes by RNA-Seq (Blueprint consortia). * P<0.05, **** P<0.0001 Wilcoxon Test.

Figure S3:

AJRCCM Articles in Press. Published July 19, 2021 as 10.1164/rccm.202101-0004OC

(A) Proportion of unique promoter-capture HiC (pcHiC) 'other ends' containing any EPIC CpGs or those identified as differentially methylated positions (DMPs) or DMRs in IPF.

(B) Proportion of all EPIC, DMPs and DMRs that are linked in 3D as determined by pcHiC. **** P<0.0001, Chi-square test with Yates correction versus all interactions containing EPIC CpGs.

(C) Number of 3D interactions per IPF DMRs (Table S3).

(D) Cell-type expression of transcription factor genes with enriched motifs in IPF DMRs in single cell RNA-Seq (scRNA-Seq) data from the IPF lung. Gene expression is projected over UMAP representation of all cell-types with brighter colours indicating more expression.

(E) Heatmap depicting average expression of DMR-associated genes in scRNA-Seq from the IPF lung across myeloid cell subtypes and healthy and IPF donors as annotated by Adams *et. al* (5).

(F) Further clustering of DMR-associated genes across myeloid cell subtypes and individual study donors. Full data available at www.ipfcellatlas.com.

Figure S4:

(A-B) Gene ontology processes and KEGG pathway enrichment analysis for all DMR-associated genes (A) and all those forming protein-protein interactions regardless of DNAm status in IPF (B).

(C) Plot depicting average DNAm across the *PFKFB3* loci for macrophage subsets (Blueprint consortia). The relative location of the IPF DMR is highlighted in red.

(D) DNAm for CpGs encompassed in the IPF DMR for macrophage subsets.

AJRCCM Articles in Press. Published July 19, 2021 as 10.1164/rccm.202101-0004OC

(E) *PFKFB3* gene expression in study AMs as determined by qPCR. ** P<0.01 Mann-Whitey Test.

(F) *PFKFB3* gene expression across single cell RNA-Seq data from the IPF lung (refer to Figure 1B) and across myeloid cell subtypes. Adams *et. al(*5) identified significant differences in *PFKFB3* expression between healthy and IPF for cells annotated as non-classical monocytes and macrophages. *** P<0.001 Wilcox Rank FDR.

(G) *PFKFB3* gene expression in macrophage subsets as determined RNA-Seq. ** P<0.01, *** P<0.001 Mann-Whitey Test.

AJRCCM Articles in Press. Published July 19, 2021 as 10.1164/rccm.202101-0004OC

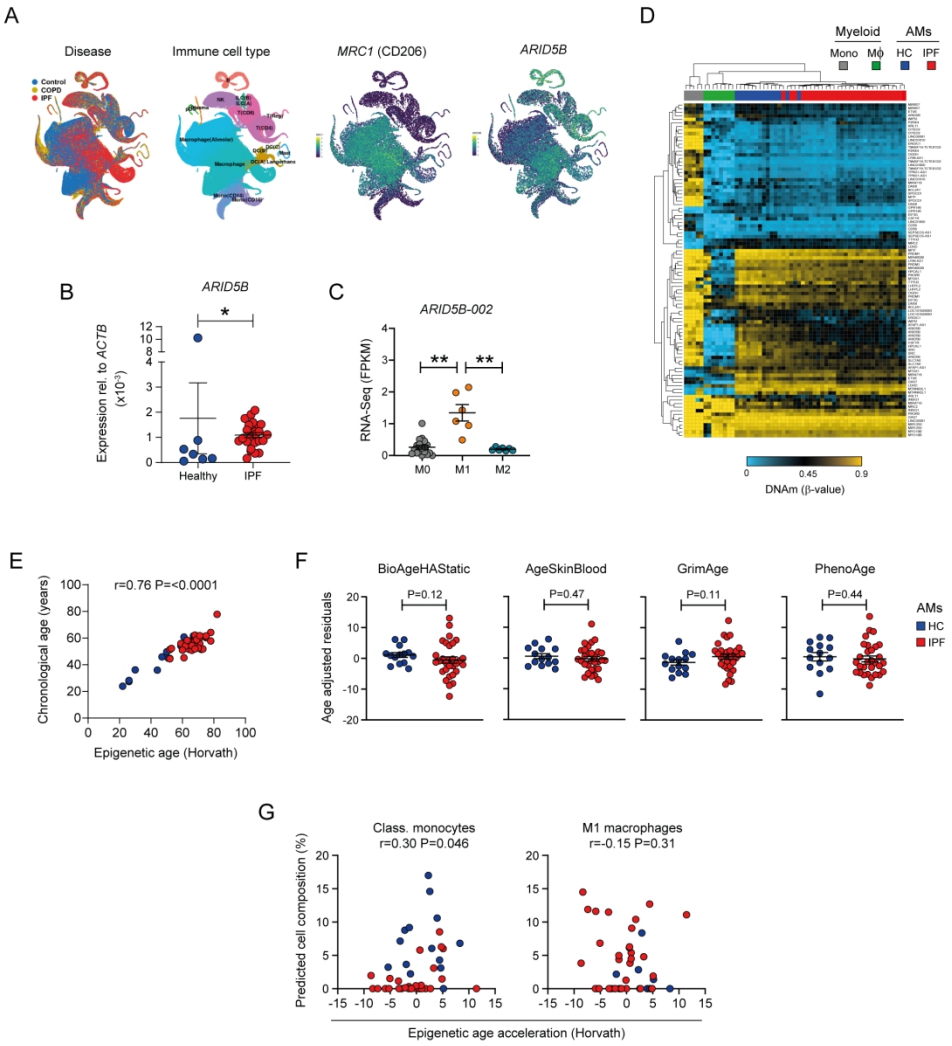

Figure S1

AJRCCM Articles in Press. Published July 19, 2021 as 10.1164/rccm.202101-0004OC

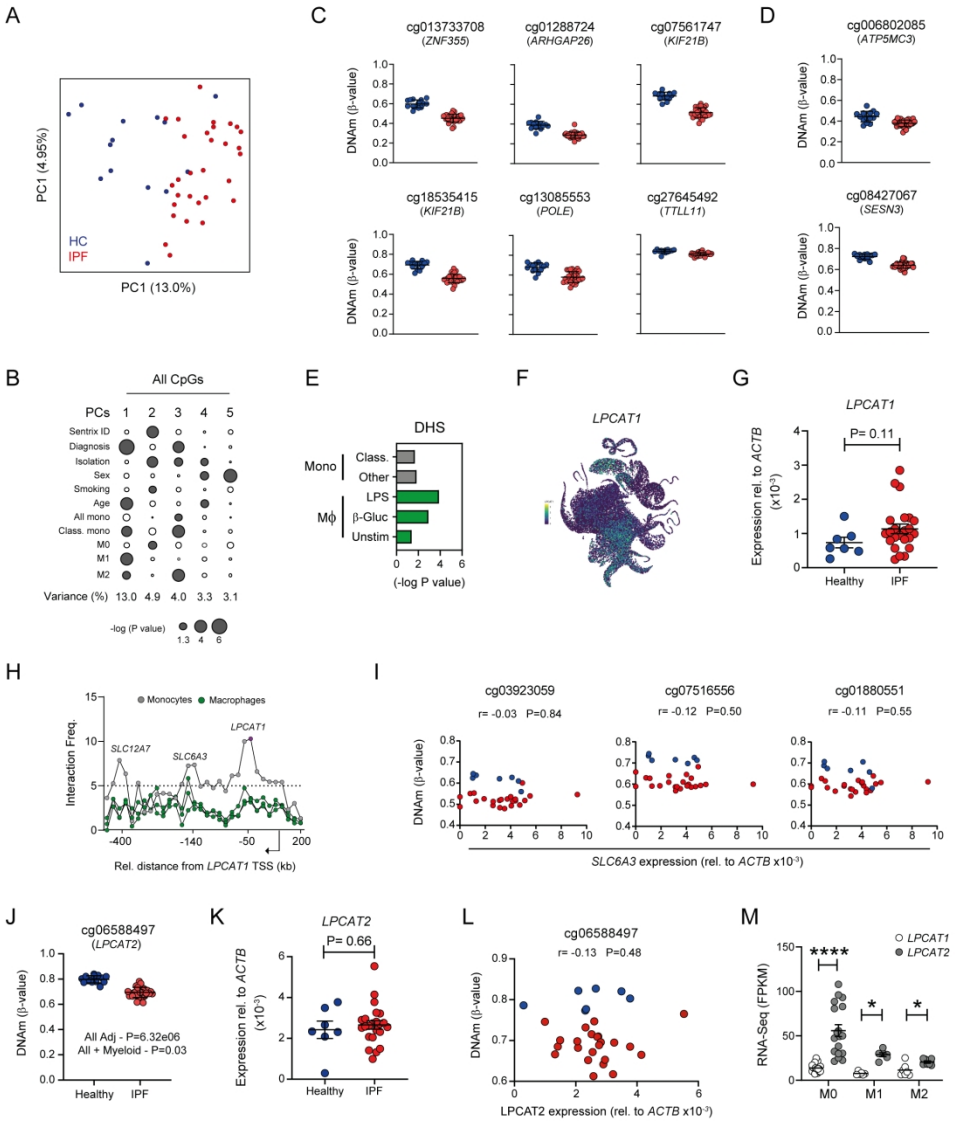

Figure S2

AJRCCM Articles in Press. Published July 19, 2021 as 10.1164/rccm.202101-0004OC

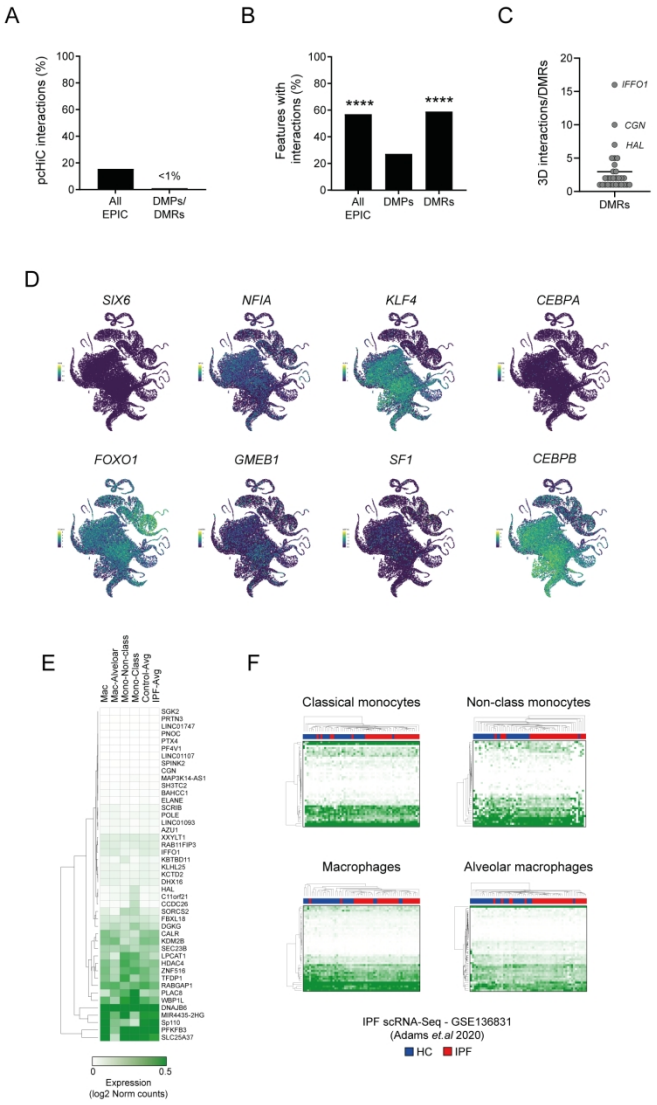

Figure S3

AJRCCM Articles in Press. Published July 19, 2021 as 10.1164/rccm.202101-0004OC

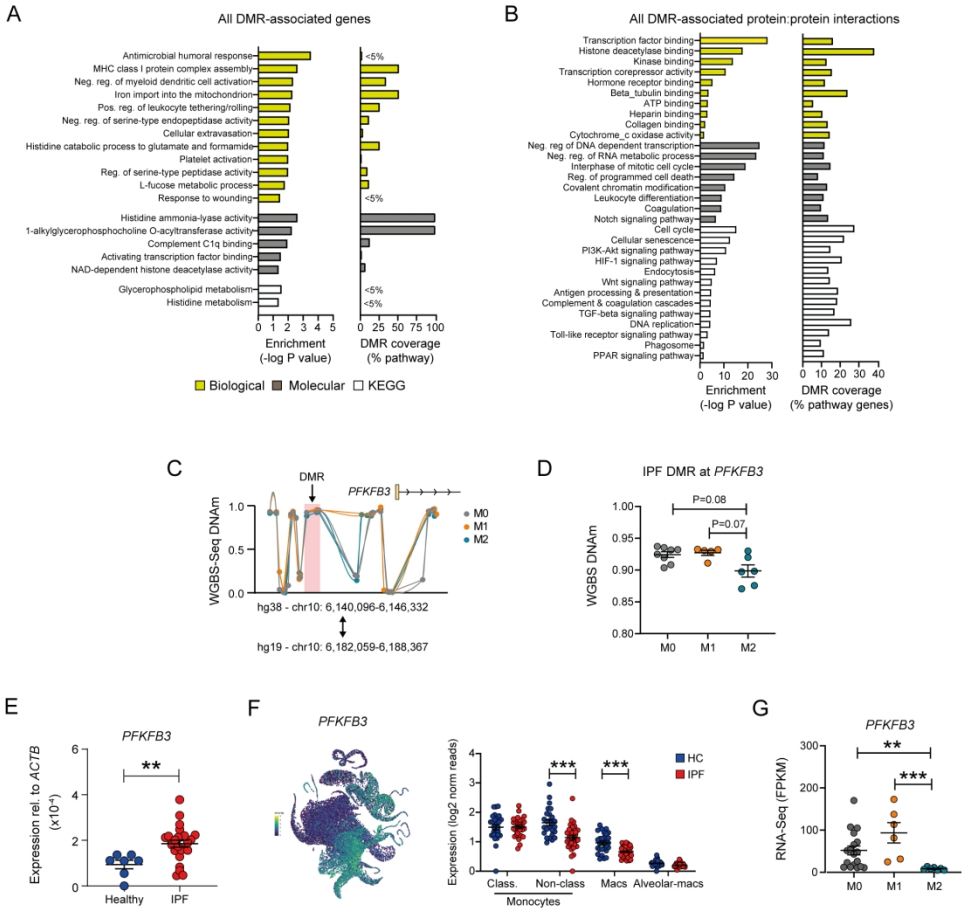

Figure S4

AJRCCM Articles in Press. Published July 19, 2021 as 10.1164/rccm.202101-0004OC